**ISTANBUL TECHNICAL UNIVERSITY ★ GRADUATE SCHOOL OF SCIENCE ENGINEERING AND TECHNOLOGY**

# DESIGN AND IMPLEMENTATION OF A DOUBLE-SIDED CORELESS LINEAR MOTOR

**M.Sc. THESIS**

**Ozge TASKIN**

**Department of Mechatronics Engineering**

**Mechatronics Engineering Programme**

**JUNE 2015**

**ISTANBUL TECHNICAL UNIVERSITY ★ GRADUATE SCHOOL OF SCIENCE ENGINEERING AND TECHNOLOGY**

# DESIGN AND IMPLEMENTATION OF A DOUBLE-SIDED CORELESS LINEAR MOTOR

**M.Sc. THESIS**

**Ozge TASKIN**
**(518101069)**

**Department of Mechatronics Engineering**

**Mechatronics Engineering Programme**

**Thesis Advisor: Assoc. Prof. Dr. Ozgur USTUN**

**JUNE 2015**

**İSTANBUL TEKNİK ÜNİVERSİTESİ ★ FEN BİLİMLERİ ENSTİTÜSÜ**

# ÇİFT TARAFLI HAVA ÇEKİRDEKLİ LİNEER MOTOR TASARIMI VE GERÇEKLENMESİ

**YÜKSEK LİSANS TEZİ**

**Özge TAŞKIN**
**(518101069)**

**Mekatronik Mühendisliği Anabilim Dalı**

**Mekatronik Mühendisliği Programı**

**Tez Danışmanı: Doç. Dr. Özgür ÜSTÜN**

**HAZIRAN 2015**

**Ozge Taskin**, a **M.Sc.** student of ITU **Graduate School of Science Engineering And Technology** student ID **518101069**, successfully defended the **thesis** entitled **"DESIGN AND IMPLEMENTATION OF A DOUBLE-SIDED CORELESS LINEAR MOTOR"**, which she prepared after fulfilling the requirements specified in the associated legislations, before the jury whose signatures are below.

| | | |
|---|---|---|
| **Thesis Advisor :** | **Assoc. Prof. Dr. Ozgur USTUN**<br>İstanbul Technical University | ..... |
| **Jury Members :** | **Prof. Dr. Ata MUGAN**<br>İstanbul Technical University | ..... |
| | **Assist. Prof. Dr. Salih Baris OZTURK**<br>Okan University | ..... |

**Date of Submission : 4 May 2015**
**Date of Defense : 4 June 2015**

***To happiness***

## FOREWORD

This thesis describes all the steps to design a coreless double-sided linear motor by using the software ANSYS-Maxwell. The goal is to design a double-sided coreless linear motor to get a better force characteristics with precise control, then compare the tests of the design with the simulation results.

By the given chance I would like to thank my advisor Assoc.Prof .Dr.Özgür Üstün for his efforts and mentoring on this thesis, his patience, his advices and sharing his knowledge. I was honoured to be one of his graduate students. His courage took me forward and made me bring this thesis to an end in a short period.

Also, I would like to thank my current employer ANSYS GmbH and especially my current manager in ANSYS Inc., Olaf Hädrich, for his support and all the resources provided during my studies. His encouragement bolstered my confidence and fuelled my excitement in my work. Olaf Hädrich maintained a professional athmosphere while cultivating an approachable environment, where I could freely ask questions.

I would also like to thank to the professors in my university who made things as much easier as they can for me.

I am also grateful for all the technical help that has been provided by, M.Sc. Mert Safa Mökükcü, Gürkan Tosun and Pooria Norouzi.

To my parents: my father, Nihat Taskin who really wanted me to have this degree and my mother, Esin Taskin I give the utmost appreciation. I want to thank my sister Ipek Taskin for all her financial support, and my aunt Mualla Pehlivan who accomodated my studies in Istanbul.

Finally, I would like to thank my friends Nimet Yildirim, Ali Yildirim, Zeynep Özlem Ince, Gözde Yolal, Pinar Kunt, Anil Sahin, Tuba Ildiri, Hakan Ildiri, Arda Tuysuz for their courage and support and Julie Trempolets for always being my rock in Munich.

May 2015

Özge TASKIN
(Electrical Engineer)

**TABLE OF CONTENTS**

**Page**

**ABBREVIATIONS**

**AC** : Alternating Current
**ACPMLSM** : Air Core Permanent Magnet Linear Synchronous Motor
**BLDC** : Brushless Direct Current
**BLDCM** : Brushless Direct Current Machine
**CAD** : Computer Aided Design
**CAE** : Computer Aided Engineering
**CNC** : Computer Numerical Control
**DAPMLSM** : Double Side Air Cored Permanent Magnet Linear Servo Motor
**DC** : Direct Current
**DSLIM** : Double-Sided Linear Induction Motor
**DTC** : Direct Torque Control
**EMF** : Electromotive Force
**FE** : Finite Element
**FEA** : Finite Element Analysis
**FEM** : Finite Element Method
**FSPM** : Flux Switching Permanent Magnet
**FSPMLM** : Flux Switching Permanent Magnet Linear Motor
**GB** : Gigabyte
**GUI** : Graphical User Interface
**IEEE** : Institute of Electrical and Electronics Engineers
**LFSPM** : Linear Flux Switching Permanent Magnet
**LM** : Linear Motor
**LSRM** : Linear Switched Reluctance Motor
**MagLev** : Magnetic Levitation
**MLFSPM** : Modular Linear Flux Switching Permanent Magnet
**MMF** : Magnetomotive Force
**MOSFET** : Metal Oxide Semiconductor Field Effect Transistor
**NdFe** : Neodymium Iron
**NdFeB** : Neodymium Iron Boron
**PEC** : Power Electronic Circuit
**PM** : Permanent Magnet
**PMLSM** : Permanent Magnet Linear Synchronous Motor
**PMSM** : Permanent Magnet Synchronous Motor
**PWM** : Pulse Width Modulation
**RLES** : Ropeless Elevator System
**SLIM** : Single-Sided Linear Induction Motor
**SRM** : Switched Reluctance Motor
**1D** : One Dimensional
**2D** : Two Dimentional
**3D** : Three Dimentional

## LIST OF TABLES

**Page**

**LIST OF FIGURES**

**Page**

**DESIGN AND IMPLEMENTATION OF A DOUBLE-SIDED CORELESS LINEAR MOTOR**

## SUMMARY

The history of linear motor technology can be traced back to the 1840s. The first model made by Charles Wheatstone was inefficient and impractical. The first feasible linear motor was created by a German engineer called Alfred Zehden in 1905 to drive trains and lifts. A more fundamental model was later developed by Herman Kemper in 1935. The best example of usage of linear motors today are in Maglev trains [32] in Japan. Less than a decade ago, linear motors were only able to move 5 meters per second with straightness, load capacity and stiffness. This is a positive sign that linear motor technology is growing rapidly and is the focus of a great amount of research and development.

Linear motors are widely used in the industry as they have a simple structure and their cost to produce is becoming much lower. However, linear motors have low power factor and low efficiency [26]. Modern linear motor applications demand greater performance. The key demands of a linear motor are high acceleration, long life, low maintanence, few moving parts and precise positioning. Some of the applications include, DNA sequencing, health operations, rocket positioning etc. Therefore, precision of linear motors is becoming significantly more important.

From ideas above, the study involves to produce a brand new linear motor. It has 22 pole pairs and 6 coils, designed in a FEM tool (ANSYS-Maxwell 2015®) and has since been into production. This purpose of the thesis is to demonstrate and explain the design of a high precision double-sided coreless linear motor. Materials simiar to the existing ones are chosen from ANSYS-Maxwell library. The materials are consisting of copper, NdFe35 and Steel_1010. Like Samarium Cobalt, NdFeB ($Nd_2Fe_{14}B$) is termed as rare earth magnet. These magnets have high coercive force and can be magnetized widthwise like a ferrite magnet. Copper windings are typically chosen over aluminum windings, even though aluminum is cheaper, copper is a better conductive material. As the application is having high precision that is applicable to many industrial areas that are listed above, it is a lot easier to design and produce the linear motor as a generic motor. The total motor weighs approximately 10.5 kg. This will be the perfect motor that can be mobile and be implemented anywhere needed.

First, the electromagnetic design of the motor is performed. After the FE analysis is done using ANSYS-Maxwell software, the force value is verified by a hand calculation. The results between the two calculations are slightly different due to moving field that needs to be taken into account.

Secondly, mechanical data set is examined for the motor design. Then, the CAD drawing of the motor is given followed by analytical verification of the design and electromagnetic analysis. The production and the tests of the electric motor that is designed is explained and finally the conclusion and future investigations are discussed.

The drive circuit is a PWM circuit designed in ANSYS Maxwell Circuit Editor. The features that effect motor design are input voltage, output force and rated speed. To

maintain the best electric design for the required force, choosing the proper materials and optimizing the coils are essential.

An electrical machine is an electromechanical device that converts energy. When one investigates, when the input is electrical energy and the output is mechanical energy it works as an electrical motor. However, if the input is mechanical energy and the output is electrical energy electrical machine works as an electrical generator.

Electrical machines can be divided into two different types which are listed as Alternative Current (AC) and Direct Current (DC) electrical machines. In an AC machine, alternative current flows into the coil and creates a rotating magnetic field in the airgap. In DC machines magnetic field is created straightly. Permanent magnet brushless DC motors are named DC but thinking of their working principle they can be considered in AC machine types. The designed linear motor can be thought like a BLDC machine.

For the linear motor a special design is produced and laboratory tests are made. According to this special design, three coils would face four magnets. The design of the motor is made by computer aided software. After designing the linear motor, electromagnetic FEM analyses are made. The coils are optimized after making several analyses by using the finite element software. When the verification of the design is obtained, production is made as well as motor assembly.

There are three hall sensors exist on the original motor. The hall sensors that are currently exist on the motor are ignored for the FEM design. An approximation is made for the FEM design for these hall sensors. In the thesis, hall sensors will not be discussed under the chapter of electromagnetic simulation.

# ÇİFT TARAFLI HAVA ÇEKİRDEKLİ LİNEER MOTOR TASARIMI VE GERÇEKLENMESİ

## ÖZET

Lineer motor teknolojisi 1840'lara dayanmaktadır. Bilinen ilk model bir İngiliz mühendis olan Charles Wheatstone tarafından yapılmıştır, ancak bu model çok kullanışlı ve uygulanabilir olarak hatırlanmamaktadır. Elverişli ilk model, bir Alman mühendis olan Alfred Zehden tarafından 1905'te tasarlanmıştır. Bu model trenlerde ve asansörlerde kullanılmıştır. Uygulamalar daha da geliştirilerek en ileri şekliyle 1935'te Herman Kemper tarafından tasarlanmıştır. Yine de herşeye rağmen lineer motorun gelişimine en çok katkıda bulunan ve mucidi olarak tanınan kişi aynı zamanda Imperial College London profösörlerinden biri olan Eric Laithwaite'dir.

Günümüzde elektrik motorlarından beklentiler oldukça fazladır. Bunlardan bazıları hafiflik, kontrol edilebilirlik, doğrudan tahrik, yüksek kuvvet/moment ağırlık oranı ve düşük bakım maliyeti olarak sıralanabilir. Bu saydığımız beklentiler, lineer motorlara olan ilgiyi son zamanlarda fazlasyla arttırmıştır. Lineer motorlar üzerine yapılan çalışmalar asenkron lineer motorlarla başlamış olsa da, lineer fırçasız doğru akım makinaları kontrol edilebilirliklerin çok daha kolay olması nedeniyle asenkron motorlarlara olan bu ilgiyi ikinci plana atmayı başarmıştır.

Lineer motorlar en basit yapılarıyla, dönel bir motorun yarıçapı boyunca kesilip lineer hale getirilmiş durumu olarak tanımlanabilir. Lineer motorda momentden söz edilmez ve bu büyüklük yerini kuvvete bırakır. Lineer motorlar uzunlukları boyunca kuvvet üretirler. Kısa zamanda yüksek kuvvet değerlerine çıkabilmektedirler. Aktarma elemanlarının olmaması ve yapıları gereği bunlara ihtiyaç dahi olmaması döner hareketi lineer harekete çevirirken kaybedilen enerjiyi ortadan kaldırmaktadır. Dolayısıyla motor sürücüleri için daha hassas kontrol sağlamaktadır. Sanayide çeşitli alanlarda kullanılabilirler. Başlıca uygulama alanmaları, CNC tezgahları, robotik ve otomasyon uygulamaları, füze konumlama sistemleri, gen dizimi, konveyör sistemleri, vinç sistemleri ve manyetik levitasyon olarak sıralanabilir. Lineer motor üzerine yapılan çalışmala çoğunlukla Almanya ve Japonya'da yer almaktadır. Lineer motorların bugünkü en ileri teknolojisi, Japonya'da bir manyetik levitasyon uygulaması olan Maglev trenlerinde kullanılmaktadır. Bu tren son zamanlarda ulaştığı 600km/sa hız değeriyle dünya rekorunu kırmıştır [40]. Geçmiş uygulamalara bakıldığında, 10 yıl öncesinde bile lineer motorlar yük altında doğrusal olarak sadece 5m/sn gibi bir hızla hareket edebiliyorlardı. Bu düşünüldüğünde Japonya'daki uygulamalar lineer motor teknolojisinde devrim yaratmıştır denilebilir. Böylece pek kullanılmamakta olan lineer motor teknolojisi yeniden dünyanın ilgisini çekmeye başlamıştır.

Lineer motorlar artık günümüzde basit yapıları ve düşük maliyetleri nedeniyle endüstride yaygın olarak kullanılmaktadır, ancak güç faktörü ve veriminin çok yüksek olmaması bir dez avantaj olarak karşımıza çıkmaktadır [26]. Günümüzde lineer motor teknolojisinden beklentiler eskiye göre çok daha ileri düzeydedir. Lineer motor uygulamalarından en dikkat çekenleri gen dizimi, tıp elektroniği ve roket konumlandırma olarak listenebilir. Bu nedenle özellikle hassas konumlandırma, lineer motor teknolojisinde her geçen gün çok daha fazla önem kazanmaktadır. Hassas konumlandırma özellikle belli durumlarda fazlasıyla dikkat edilmesi gereken bir husustur. Özellikle çok yüksek ve çok düşük hız durumu, hızlı ivmelenme ve hızlı

yatışma süresi söz konusu olduğunda ön plana çıkar ve verimliliği arttır. Bu durum düzgün hareket ve aşırı hassas ayar gerektiren mekanik ve konumlama elemanlarının başlıca araştırma konusudur. Tüm bu araştırmalar esasında motorun değişken yüke ve uygulanan kontrol sinyaline çabuk cevap verebilmesini amaçlamaktadır.

Lineer motorun çalışma ilkesi Lorentz ve Faraday yasasına dayanır. Lorentz kuvvet yasası içinden akım geçirilen bir iletkenin, akıma dik olarak endüklenmiş bir manyetik alana yerleştirilmesi sonucunda bu iletkene bir kuvvet etkiyeceği ve bu kuvvetin iletkeni hareket ettirmeye çalışacağını söylemektedir. Bunun yanında bu kuvvetin iletkendeki sarım sayısı, sargı akımı ve üretilen akı ile doğru orantılı olduğu bilinmektedir. Faraday yasası ise manyetik alan içerisinde bulunan bir iletken, bu alan içerisinde belirli bir hızla haraket ettirilirse bu iletken üzerinde bir gerilim endüklendiğini söyler.

Bu fikirlerden yola çıkılarak var, tez çalışmasında yeni bir lineer motor tasarlanıp üretilmiştir. Çalışmanın amacı çift yanlı, hava çekirdekli yüksek konum hassasiyetine sahip lineer bir motor tasarlamaktır. Uygulama alanları robotik ve otomasyon uygulamaları olarak belirlenmiş ve motor jenerik olarak tasarlanmıştır. Motorun yapısı gereği tasarım amacına ulaşmaktadır. Hava çekirdekli yapı düzgün harekete olanak vermektedir. Bunun nedeni hareketli parça üzerinde fazladan manyetik yük bulunmaması ve bu yükün stator sırt demiri ile manyetik etkileşime girememesidir. Bu durum daha hassas kontrol olanağı sağlar. Çift yanlı yapı motorun çok yüksek ve çok düşük hızlarda çalışmasını ve daha hızlı ivmelenmesini sağlar. Bu durum ise tamamen çift yanlı yapının daha homojen bir alan dağılımı oluşturmasından kaynaklanır. Tasarlanan motorun problemi ısı ve kapladığı alan olarak belirlenmiştir.

Motorun önemli üç ana bölümü bulunmaktadır, bunlar; mıknatıslar, sargılar ve stator sırt demiri olarak listelenmiştir. Lineer motorda 22 kutup çifti ve 6 sargı bulunmaktadır. Tasarım ANSYS-Maxwell programında gerçekleştirilmiş, yapılan çalışmalardan sonra sonuçlar tasarıma gönderilmiştir. Çalışmanın amacı çift taraflı hava çekirdekli ve yüksek konum hassasiyetine sahip bir lineer motor tasarlamaktır. Malzeme seçimi ANSYS-Maxwell kütüphanesinden gerçekte var olan malzemelere uygun olacak biçimde yapılmıştır. Malzemeler bakır, Steel_1010 ve NdFe35 olarak seçilmiştir. Samaryum kobalt gibi NdFeB mıknatısı da nadir toprak mıknatısları arasında yer almaktadır. Bu mıknatıslar genel olarak demir, bor ve neodyum alaşımından oluşur ve kimyasal formülü $Nd_2Fe_{14}B$ olarak yazılır. Bu tip mıknatısların koersif kuvvetleri yüksek olup tıpkı ferrit mıknatıslar gibi enine mıknatıslanmaya uygundurlar. Sargılar alüminyum yerine bakır olarak seçilmiştir. Bakırın en iyi iletken olması bu kararda önemli rol oynamıştır. Tez çalışması yüksek hassasiyette bir lineer motor tasarlamak olup, bu uygulamanın endüstride bir çok alanda kullanılmasından dolayı iç parçalar ve bağlantı parçalarının jenerik olarak üretilmesine karar verilmiştir. Toplam motor ağırlığı 10.5 kg'dır. Hafif olması nedeniyle birçok yerde kullanılabilir ve taşıma kolaylığı sayesinde istenilen yere monte edilebilir.

Elektriksel tasarımı motorun manyetik analizleri ve kontrol devresinin tasarlanması oluşturmaktadır. Bu tez çalışmasında sadece motorun elektrik, manyetik tasarımı ve üretimi anlatılmaktadır.

Öncelikle motorun mekanik hesapları yapılmış ve bu hesplara dayanılarak motorun üç boyutlu çizimi gerçekleştirilmiştir. Üç boyutlu çizimden sonra analitik ve sonlu elemanlar yöntemi kullanılarak iki boyutlu elektromanyetik hesaplarla motor tasarıma hazırlanmıştır. Bunu takiben motor üretimi gerçekleştirilmiş ve motor

testlerine başlanmıştır. Motor tesleri ile sonlu elemanlar analizi arasında büyük tutarlılık görülmüştür. Tezin sonunda sonuçlar ve gelecekteki çalışmalar bölümüne yer verilmiş ve bu konudaki düşünceler belirtilmiştir.

Sonlu elemanlar yöntemiyle motor tasarlandıktan sonra ilk olarak kuvvet hesabı el hesabı ile tekrar kontrol edilmiş ve analiz sonucu doğrulanmıştır. Ortaya çıkan ufak fark nümerik olup hata sınırları içerisinde kalmıştır.

Sürücü devresi bir PWM devresi olup Maxwell Circuit Editor programında tasarlanmıştır. Motor tasarımını etkileyen faktörler giriş gerilimi, çıkış gücü ve anma hızı olarak bulunmuştur. Gerekli güç için en iyi tasarımı elde etmek doğru malzeme seçimi ve sargı optimizasyonu ile olmaktadır.

Elektrik makinaları elektromekanik enerji dönüşümü yapan aygıtlardır. Elektrik enerjisi verilip mekanik enerji alınıyorsa buna motor çalışma, mekanik enerji verilip elektrik enerjisi alınıyorsa da buna jeneratör çalışma denmektedir.

Elektrik makinaları iki ana başlık altında incelenebilir. Bunlar doğru akım ve alternatif akım makinaları olarak adlandırılabilir. Alternatif akım makinelerinin çalışma prensibi alternatif akımın sargılardan geçmesi ve hava aralığında döner alan oluşturması prensibine dayanır. Alternatif akım makinalarının alt dallarına bakılacak olursa senkron ve asenkron makinaları karşımıza çıkar. Senkron makinalar altında ise fırçasız doğru akım makinası bulunur. Doğru akım makinalarında ise manyetik alan doğrudan oluşur. Doğru akım makinaları komutasyon ve homopolar olarak iki ana gruba ayrılır. Komutasyon ile çalışan motorlardan biri de sabit mıknatıslı makinadır.Yani sabit mıknatıslı makinalar doğru veya alternatif akımla çalışabilir. Sabit mıknatıslı doğru akım makinaları adında doğru akım bulundursa da aslında alternatif akım makinaları altında yer almaktadırlar. Tasarlanan lineer motor fırçasız doğru akım makinası özelliklerini taşımaktadır. Endüklenen gerilimi ise sabit mıknatıslı senkron makinaya benzer.

Bunun yanında lineer motorların tasarımlarına ilişkin özel sınıflandırmaları da bulunmaktadır. Örneğin, fırça tipine göre fırçalı ya da fırçasız lineer motorlar; stator şekline göre tüp şeklinde, çift yanlı ya da yassı lineer motorlar; çekirdek tipine göre ise demir çekirdekli, hava çekirdekli ve slotsu lineer motorlar olarak sıralanabilir. Tasarlanan lineer motor her grubun bir özelliğine sahip olmak üzere fırçasız, çift yanlı ve hava çekirdekli olarak bu listede yerini alır.

Tasarlanan lineer motor sargıları üzerinde önemli optimizasyon çalışmaları yapılmıştır. Sonuçta üretilen motordaki tasarımda 4 mıknatısın karşısında 3 sargı olacak şekilde bir düzenleme yapılmış ve bunun diğer çalışmalarla kıyaslandığında en yüksek kuvvet değerini oluşturduğu görülmüştür. Motor tasarımının her aşaması sırasında bir bilgisayar programından yararlanılmıştır. Analizler sonlu elemanlar yöntemiyle yapılmıştır ve sargılar bu yöntemle yapılan analizler sonucunda optimize edilmiştir. Yapılan tetkiklerden sonra, motor üretimi ve montajı gerçekleştirilmiştir.

# 1. INTRODUCTION

Linear motor technology dates back to the 1840s. Stepper motors and brushed linear motor products have been available for quite some time. The brushed system of a DC motor was expensive and limited. By the time, the control technology became more powerful, brush commutator systems were withdrawn and this opened the way to BLDC and linear motors.

The basic principle behind the linear motor was discovered in 1895, but practical devices were not developed until 1947. In the 1950s, the British electrical engineer, Eric Laithwaite, started to consider whether linear motors could be used in electric weaving machines. Laithwaite's research at Imperial College in London, attracted international recognition in the 1960s. This was followed by a speech at the Royal Institution named "Electrical Machines of the Future".

Today, linear motors are used in various applications that require linear motion, including overhead traveling cranes and beltless conveyors for moving sheet metal. Linear motors are best known as the source of motive power in the latest generation of high-speed "maglev" trains which recently broke the world's speed record [40]. This concept is illustrated in Figure 1.1. Maglev trains promise safe travel at very high speeds. They are, however, expensive and incompatible with the current railroads. Most research on Maglev trains has been carried out in Japan and in Germany.

**Figure 1.1 :** Prototype Maglev railroad test, 2001 by NASA [38]

Today's linear motion applications are more demanding than ever. Faster throughput, more exact positioning, longer life, less maintenance and fewer moving parts are some of their requirements. Motion control companies strive to meet and exceed these requirements by continuing technological advancement.

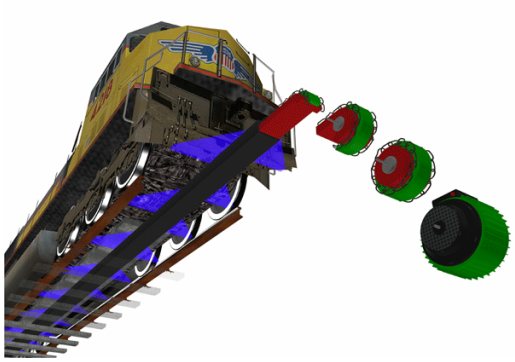

**Figure 1.2 :** Illustration of linear motion on a train movement [39]

Less than a decade ago, it was difficult to find a commercially available linear bearing that could travel 5 meters per second with straightness, load capacity and stiffness. Today, there are many linear bearings with these attributes and they are fairly cost effective.

In a traditional DC electric motor, a central core of tightly wrapped magnetic material spins at high speed between the fixed poles of a magnet when an electric current is applied. In an AC induction motor, electromagnets positioned around the edge of the motor are used to generate a rotating magnetic field in the central space between them. This induces electric current in a rotor, causing it to spin. A linear motor is effectively an AC induction motor that has been cut open and unwrapped. Hence, they do not have any rotational motion and the general idea of it is simple enough, as is depicted in Figure 1.3.

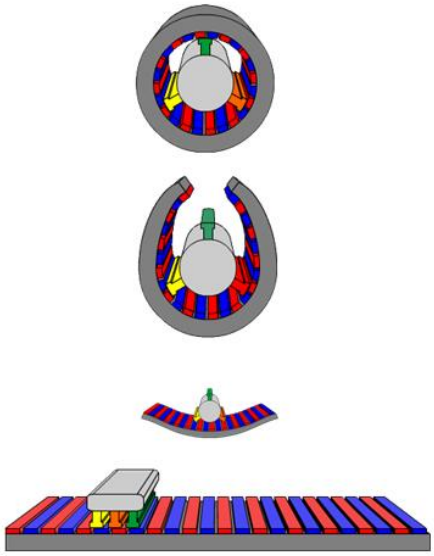

**Figure 1.3 :** Unwrapping a rotational motor will make a linear motor [41].

Linear motors are electric induction motors that produce motion in a straight line rather than rotational motion. The stator is laid out in the form of a track of flat coils made of aluminum or copper and is known as the primary of a linear motor. The rotor takes the form of a moving platform, is known as the secondary. When the current is switched on, the secondary glides past the primary, supported and propelled by a magnetic field.

A linear motor consists of a moveable vehicle and a stationary rail part as shown in Figure 1.4. Considering the forcer as a stator (stationary part) and the coils as a rotor (moving part) makes a good model for a linear motor structure. This design creates a direct connection between the load and the motor.

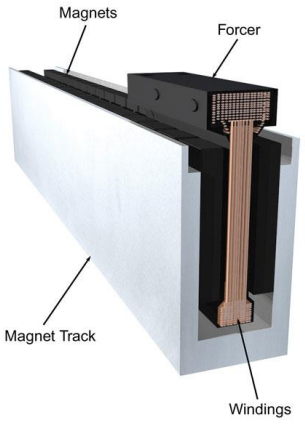


**Figure 1.4 :** Linear motor structure [42].

When currents are applied to the motor, force is produced. The created force will make the rotor move with a velocity of *v* and the rotor slides throughout the x-axis according to the magnetism of the system. The direction of the movement is determined due to the applied currents and their directions.

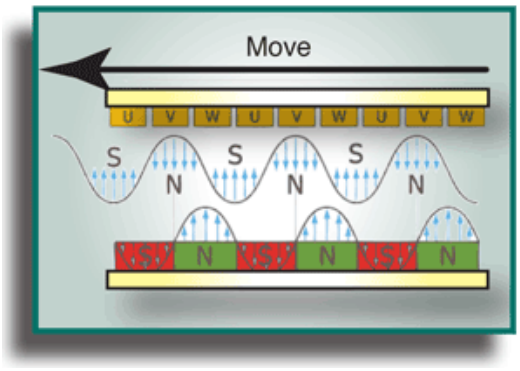


**Figure 1.5 :** Movement of the rotor [43].

The basic physical principle behind the linear motor design is the Lorentz force law. This law states that the amount of force (F) a motor can generate is equal to the magnetic field density (B) vector cross product (X) times the length of wire in the wire spool (L) multiplied by the amount of the current (I) in the winding. To develop a more efficient linear motor, the amount of current (I) must be reduced by maintaining the same force output. The remaining variables of Lorentz force law must be maximized to increase the efficiency of the motor design.

Several types of linear motors are available in the market with different ways of classification. They can be classified according to their brurshes (e.g., linear motors with brushes and brushless linear motors). An example of a linear motor with brushes can be seen below.

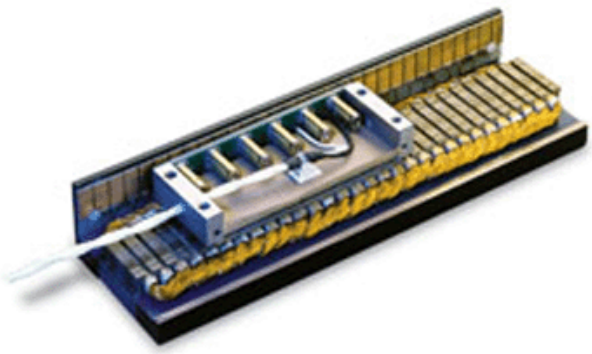

**Figure 1.6 :** Linear motor with brushes [37].

According to their shape, they are classified as tubular, U-channel or plane linear motors. An example of a U-channel linear motor can be seen in Figure 1.7.

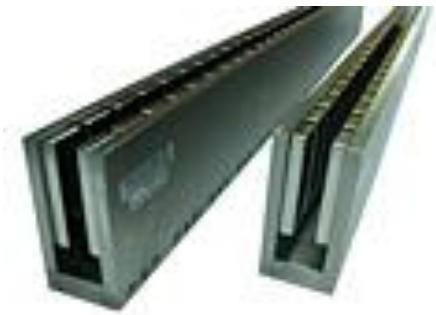

**Figure 1.7 :** U-channel linear motors [44].

According to their core structure, they are classified as iron core, aircore or slotless linear motors.

Linear motor benefits can be listed as:

- High speed
- High precision
- Fast response
- Stiffness
- Zero blacklash (no transmission components)
- Maintanence free operation

The down sides of linear motors are:

- Cost
- Higher bandwidth drives and controls
- Force per package size (they are not compact force generators)
- Heating
- No (minimal) friction

The main problem with linear motors have always been the cost and the difficulty of developing suitable electromagnets. Enormously powerful electromagnets are required to levitate and move big structures, and these typically consume substantial amounts of electric power. Superconducting magnets are used to solve this problem.

Every linear motor type has its own advantage. Below is a summary of linear motor attributes and how each type of motor compares to the others.

**Table 1.1:** Linear motor types and comparison of their attributes.

| Attribute | Iron Core | Air Core | Slotless |
|---|---|---|---|
| Cost | Low | High | Lowest |
| Attractive Force | Highest | None | Moderate |
| Cogging | Highest | None | Moderate |
| Force / Size | Best | Moderate | Good |
| Thermal Characteristics | Best | Worst | Good |
| Forcer Weight | Heaviest | Lightest | Moderate |
| Forcer Strength | Best | Worst | Good |

In this thesis, a double-sided coreless linear motor is designed. Double-sided, coreless linear motors can work in very high and very low speeds, they can accelerate faster, they are low maintenance and they do not have parts that reduce the efficiency (e.g. rollers).

However, they also have disadvantages. For example, they are not very efficient in vertical applications, they do not have an emergency brake and they are not handy in linear encoder applications considering the environmental conditions.

Despite these disadvantages, double-sided coreless linear motors are widely used in industry settings. The most common areas are:

1) Conveyor systems
2) High precision direct drive systems
3) High precision control with higher speeds

An example of a conveyor system built with double-sided coreless linear motor can be seen in Figure 1.8. In the figure, two double-sided modular linear motor systems are used to move a carrier. They are synchronized in their actions. As there is no conversion of rotational motion to linear motion, the design is more force efficient than a traditional DC motor.

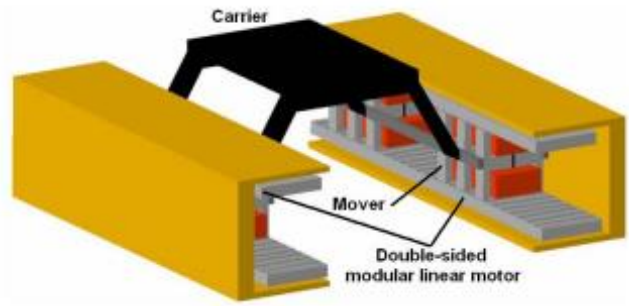


**Figure 1.8 :** Sample double-sided coreless linear motor application [46].

## 2. LITERATURE REVIEW

As the linear motor technology becomes more popular, it has been successfully applied in many different industries (e.g., in health, defense and aerospace). These new applications introduced new challenges in the design, modeling and analysis of linear motors. Many studies indicate that FEM software is well suited to obtain adequate models of the motor. The following articles from IEEE have been taken into consideration for the literature review.

In the year 2013, the paper "*Investigation and general design principle of a new series of complementary and modular linear FSPM motors*" compared the conventional FSLM and rotary FSLM. It is indicated that, conventional FSLM has unbalanced magnetic circuit at the end of the coil, as well as having greater cogging force and force ripple. FEM is used for different mover/stator pole pitch ratios to reduce cogging force and thrust force ripple to validate the experimental results. General design principles for MLFSPM motors with different pole pitch ratios are concluded [3].

In the paper "*A new modular and complementary double-sided linear flux-switching permanent magnet motor with yokeless secondary*" which was published in 2014 in the 17$^{th}$ International Conference on Electrical Machines and Systems, R. Cao, W. Huang and M. Cheng studied a LFSPM which has both the armature windings and the magnets in the short double-sided primary mover. The long stator consists only of a yokeless iron core. They compared single and double-sided motor and proved that the proposed motor is more advantageous. It has a lower secondary, a higher power density, smaller friction forces and is overall more efficient. It is seen that the motor is especially suitable for long stator applications such as, urban rail transit and elevators in high buildings. The calculations are made using FEA [4].

In 2012, A. Buarse, and W. Subsingha published the paper "*Double-sided linear induction motor control using space vector pulse width modulation technique* " in the 10$^{th}$ Eco-Energy and Materials Science and Engineering conference. They presented

a DSLIM that has 500W, 300 Vmax, 50 Hz power rating. The used control technique is the average Space Vector Pulse Width Modulation that is applied on a 3 Phase Voltage Source Inverter. A real time control interfacing board (DS1104) was used from dSPACE and utilized by the software development kit Matlab/Simulink. The controller design has been successfully validated by experiments. Both motor speed and rotational controller of the DSLIM were tested with the 3 phase voltage source inverter [2].

In the energy conference ENERGYCON in 2014 in Dubrovnik, M. Caruso, G. Cipriani, V. Di Dio, R. Miceli and C. Sparataro have discussed "*Speed control of double-sided linear induction motors for automated manufacturing systems*". They presented the modeling, simulation and determination of the parameters of a double-sided linear induction motor. They showed that DLIM is gaining more importance in automated manufacturing systems. A constant voltage/frequency speed control system is used in the study. They verified the performance of the motor on a test bench. Simulation and test results show a good agreement and that the speed control system is succefully validated [5].

In 2015, Hsin-Han Chiang and Kou-Cheng Hsu studied the motion control of a LIM drive in their work "*Optimized adaptive motion control through an SoPC implementation for linear induction motor drives*". They proposed an optimal adaptive tracking control for a LIM drive. They took end effects, payloads and model uncertainties, e.g., friction force, into account. They used a field-oriented control for a LIM and first investigated the primary end effects in the dynamic model. For the basis of the back stepping control design, they embedded a sliding mode controller with a particular fuzzy compensator to deal with the lump uncertainities of the LIM drive. To overcome the obstacle of the unknown bounds of the lumped uncertainities in the total system, an adaptive mechanism is derived to adjust the fuzzy compensator gains. They achieved robust tracking performance in existence of uncertainities and nonlinearities by adopting the soft computing technique and optimizing the controller parameters. Finally, the high performance of the proposed control scheme is validated by hardware experiments [6].

M.J. Chung and D.G.Gweon published the paper "*Design optimization and development of linear brushless permanent magnet motor*" in 2003. This paper introduced a design optimization for minimization of force ripple and maximization

of thrust force in a linear brushless permanent magnet motor. In this paper, no FEA is represented but the sequential quadratic programing method. It is proven that by using this method, the normalized force ripple is reduced 7.7% and the thrust force is increased 12.88N compared to non-optimized designs [7].

The paper "*A new double sided linear switched reluctance motor with low cost*" which was published in 2006 by F. Daldaban, and N. Ustkoyuncu, showed a design of a new LSRM structure. As described in the paper, this model used double-sided configuration. There was a 3m experimental road and a translator that has a weight of 7.5 kg. LSRM was driven by three asymmetric MOSFETs with a 30 VDC voltage supply. This configuration created a higher force with lower cost for many industrial applications. A FEA of the motor was conducted and compared with the test results. The paper indicates that the FEA is correlated with experimental results, which is around 99% [8].

The paper "*Efficiency maximization of the air core double-sided permanent magnet linear synchronous motor*" has been published by A. Darabi, R.Ghanaee, A. Shariati, and M. Siahi, in 2013. They recommended ACPMLSM for applications where accurate control of speed and postion is required. In the paper, it is proven that the omission of the core in the primary of the motor reduces the detent force and increases the controllability of the motor. In the paper, the FEM and Maxwell's equations are used to calculate the flux density of different parts of the motor. It is visible that a precise flux density model is presented and ACPMLSM is optimized for the efficiency maximization by using a genetic algorithm [9].

Dr. G.W. McLean has published "*Review of recent progress in linear motors*" and discussed the recent advances in linear electric machines. He has described the use of linear machines for industrial purposes. He has given a report of their application to transport propulsion and levitation. Several types of linear motor developments were described. He has provided a description of most major experimental and implemented transport projects using linear motors, along with the reported performances of the different arrangements. The paper concludes with a review of the analytical techniques used to obtain the performance of linear machines. He has given a description of direct-solution layer methods and FEM techniques with a comparison of accuracies achieved by each method [10].

In the paper "*Control strategies for linear synchronous motors*" Dr. Brian M. Perrault discussed advantages and disadvantages of linear motors and their control strategies. He stated that linear motors are superior to the other means of propulsion, as the force is applied directly to the vehicle, does not depend upon friction, is controllable, and the linear motors themselves have no wearing parts. He indicated the unique challenges of linear motors, such as the back-emf, can vary with position as well as speed, the overall thrust constant can vary if there are gaps between the stators, and the stators must be synchronized as a vehicle transition from one to the other. To manage these charatersitics the importance of stator length that is energized is indicated. Perrault also discussed methods for operating multiple vehicles safely under the constraints of linear motor block-based control [11].

In 2013, Lei Huang, Haitao Yu, Minqiang Hu and Hexiang Liu have published a paper "*Study on a long primary flux switching permanent magnet linear motor for electromagnetic launch systems*". In their work, they developed a FSPMLM model based on the principle of rotational flux switching permanent magnet machines. They indicated that, it is more suitable for EMLS because of having high thrust density and a simple structure of the secondary. The study consisted of several steps. First, they analyzed the structure and operation principle of the proposed FSPMLM and secondly thrust compoments are analyzed and derived considering the longitudinal end effect. The goal was to reduce the thrust ripple. A 2D transient model solved by FEM was employed to investigate the dynamic electromagnetic characteristics of the FSPMLM and the process of electromagnetic launch. To validate the thrust performance a prototype of a single-sided FSMLM was used [12].

*"Analytical framework for thrust enhancement in permanent-magnet (PM) linear synchronous motors with segmented PM poles"* was published by Arash Hassanpour in 2010 to discuss the usability of segmented permanent magnet poles. The goal of his study was to see if an accurate analytical model of a coreless double-sided linear permanent-magnet motor with segmented permanent-magnets poles was feasible. In the proposed model the thrust average and thrust ripple was precisely predicted. Back electromotive force and flux density distribution of the motor was also determined. He chose the finite element method to verify the results and optimized the pole dimensions by using the proposed model and generic algorithm. The goals of the optimization were the minimization of the thrust mean and thrust ripple. This model

provided an analytical framework for design and optimizaion of motor parameters under various objectives [13].

X. Jin, M. Weiming, Z. Yuxing and S. Zhaolong published a paper in year 2014 called *"Nonlinear calculation methods of long primary double-sided linear induction motor"*. The purpose of the paper was to investigate a slotless double-sided long-stator linear induction motor for the application of electromagnetic launch. There were several modifications of the motor. For example, the conventional gullet structure was cancelled and the conductive area of the motor stator winding was enlarged which decreased the loss and temperature rise. Simulations were performed by using FEM to obtain saturation characteristics of the stator leakage and excitation inductance. Experimental and simulation results were compared and this verified the validity of the proposed calculation method [14].

Another paper from X. Jin, M. Weimming, L. Junyong, S. Zhaolong and Z. Yuexing called "*The mathematical model and performance analysis of a novel four-stator double-sided linear induction motor*" was written to design an electromagnetic aircraft launch and the electromagnetic model for this study was presented in this paper. The coupling characteristics of inductive loop on the shuttle inducted by the upper and lower stators, and the coupling characteristics of adjacent windings of the upper and lower stator-ends were analyzed in detail. Based on the advanced equivalent coupling circuit model, the coupling characteristics of relevant physical quantities of the upper and lower stator and lower equivalent windings of shuttle were studied. Moreover, they derived the relationship between the cooling charateristics and motor operation conditions. Experiment results verified the validity of the proposed design and analysis methods [15].

In 2004 J. J. Kim, Y. H. Jeong and D. W. Cho published "*Thermal behavior of a machine tool equipped with linear motors*". In their work, the goal was to show the thermal behavior of a motor by using a FEM tool. They supported the idea of development of a feed drive system with high speed and accuracy which has been a major issue in the machine tool industry. They also mentioned that the high speed feed drive system with linear motors in return generates heat problems, specifically, frictional heat is produced at the ball or roller bearing of the LM block when driven at high speeds. In the paper, the thermal deformation characteristics were identified through measuring the thermal error caused by the thermal deformation of the linear

scale and machine tool structure. They used FEM to identify the dominant thermal error components and showed that the proposed analysis scheme is efficient in identifying the dominant thermal error components and its magnitudes [17].

In the paper "*Performance comparison of control methods for high speed long primary double-sided linear induction motor*" a LIM and long primary DSLIM are investigated for high-speed linear motor application. It was hard to detect the secondary speed with high-accuracy and fast response. The paper compared two control methods for the performance of the long primary DSLIM. The two methods were direct thrust control and secondary field oriented control. The simulation results for both control methods were compared based on motor performance. It was discovered that it is difficult to detect the fast response and high-accuracy secondary speed for the long primary DSLIM in high-speed applications. It was proven that without the high-accuracy and fast response of the secondary speed feedback, the performance requirements can be obtained through the direct thrust control method [18].

The paper "*Direct force control for a three-phase double-sided linear induction machine with transverse magnetic flux*" published by Roberto H. Manno and Eduardo Galvan Diez, investigated symmetrical rotary induction machines. DTC is known as being used widely for those kind of machine analysis. The paper extends the conventional rotary motor theory to LIM analysis. They designed and developed a LIM model to compare experimental test results and the simulation results [19].

*"Design method and analysis of double-side air-core permanent magnet linear servo motor"* which was published in the International Conference on Electrical Machines and Systems (ICEMS) 2010, analyzed the magnetic field of DAPMLSM by using EMI. With accurate FEA results, the formulas and experimental results were proven. The results were used to analyze no-load magnetic harmonics to reduce thrust ripple. Changing the winding pitch and current order, they gained more stable thrust which indicated that the harmonics from a non-sinusoidal magnetic field and end effects of a linear motor are equal. The goal was to obtain optimal sinusoidal magnetic field and stable thrust. To reach that goal, the design laws for the motor's main dimensions, including windings, were discussed [20].

M. Mirsalim, A. Droudi and J. S. Moghani have published the paper "*Obtaining the operating characteristics of linear motors: a new approach*" in 2002. They modified the suggested Duncan LIM by using FEM and simulation. There were several changes of the new modified motor. The paper discussed special phenomena in linear motors such as transverse edge effect, longitudinal end effect and saturation of back iron. They first computed the saturation by simple equations and iterative methods. By FEA they computed equivalent circuit parameters. The Duncan model is used to take the end effects into account. They proved that the modified model accurately represented an LIM. They changed the equivalent circuit parameters to take different operating conditions into account. Finally, they compared the simulation results with experimental measurements to validate the accuracy of the proposed model [21].

"*Precise position control of tubular linear motors with neural networks and composite learning*" is a paper that takes into account uncertinities like friction and electromagnetic phenomena and approximates these with a radial basis function neural network which is trained online using a learning law based on Lyapunov design. This study examines an adaptive control scheme with micro-metric positioning tolerances. The approximator is trained using a composite adaptation law combining the tracking error and the model prediction error. Study shows that a precise control is possible [22].

In the paper "*Force measurements on a shielded coreless linear permanent magnet motor*", K. J. W. Pluk, J. W. Jansen and E. A. Lomonova compared the force measurements on a shielded coreless linear motor with 2D models. Their study applied a semianalytical modeling method based on Fourier modeling and included force calculations. The semianalytical modeling method was able to predict the behavior found in their measurements, however, saturation effects in the shield were ignored. They proved the measurements match with the semianalytical modeling method [23].

In their paper "*Reducing pitch error of a linear motion system actuated by a permanent magnet open face linear motor*" G. Rotenhoefer and A. Slocum discussed iron-core open face linear motors. In this type of motor, the magnetic attraction between forcer and magnet track was about 5-7 times higher than the maximum motor force. They stated that the magnetic attraction can be used in different bearing concepts. The problem in the paper is described as attraction force, creating a pitch

moment and resulting position dependent, periodic pitch error motion because of finite bearing stifness. However, it can still be seen that a high-precision grinding tool machine was successfully introduced [24].

One of the most important problems in these technologies is precise control. K. Sato in 2014, published a paper called "*High-precision and high-positioning of 100 G linear synchronous motor*" to indicate that linear motors can move with an acceleration above 100G, while also being capable of high-precision and high-speed positioning with a velocity of 12m/s that can provide up to 500nm of position accuracy [25].

"*A full scale superconducting magnetic levitation (MagLev) vehicle operational line*" was presented in 2015 which described the construction and main components of a MagLev vehicle. The work was done in Rio de Janerio for connection road inside the campus of Federal Universiy of Rio de Janerio with a 200m long lane. It took 13 years to finish the project. The actual vehicle was 1 ton and designed to transport up to 24 passengers. NdFeB was chosen for the magnet material so that the superconductors would be able to overcome high temperatures. Regenerative breaking with the automatic supply system of liquid nitrogen was presented in the paper [27].

R.K. Srivastava from the Department of Electrical Engineering in the Institute of Technology of Banaras Hindu University mentioned the precision of FEA and simulation approaches in his paper "*Characteristics of double gap SLIM under constant current excitation*". He also discussed how to develop a double airgap five-layer Fourier transform model of SLIM and a prediction of its performance in the Fourier-space using Parseval's theorem. He later developed a model by using ANSYS 5.0 FEM code to validate the experimental results. It was seen that even though FEM results were slightly overestimated, the measured results show strong correlation with computed results both in FEM and from the Fourier transform analyses [28].

Ozgur Ustun, Guven Komurgoz and Nejat Tuncay published a paper "*Sürekli mıknatıslı demir çekirdeksiz lineer fırçasız doğru akım motoru tasarımi*" about permanent magnet air-core linear brushless DC motors. As the industry began to require more efficient electrical machines, linear brushless DC motor designs became

lighter, started to create greater force, have smooth motion capability, allowed direct load driving and greater controllability. Thet indicated new generation electric machine designs are application-oriented and modulated for operation conditions in linear motors and most studies on linear motors are made on linear induction motors. They mentioned after the new developments on electronic components and magnetic materials, an interest grew in brushless DC linear machines. They also stated that DC linear machines have very good operation characteristics and control capability. They discussed the improvement for electrical machines is on coreless motors with coggingless behavior for smooth motion applications. The paper described the design and production of a linear coreless brushless DC motor consisting of three main parts, as permanent magnets (strontium-ferrites), three phase windings and back irons. They explained that linear motion is performed by the interaction between two magnetic circuits constructed by permanent magnets and back iron having coreless windings. FEM analysis and the experimental results were also included in the paper [29].

The paper "*Design, analysis and control of a novel linear actuator*" which was published in 2006 by O. Ustun, and R. N. Tuncay, discussed developing a linear actuator for accurate position control with high force to mass ratio. They developed a new double sided motor by using NdFeB magnets which had a printed circuit moving armature. They used finite element analysis to perform the simulations and predict performance of the motor. They introduced a new criteria for design optimization. They developed a hardware in the loop control technique and applied to the motor. In the paper, it is explained that micrometer position accuracy is achieved experimentally and the experimental values are in good agreement with the computational values [30].

Tong Yang, Libing Zhou and Langru Li calculated the performance of a DLIM with short secondary in "*Performance calculation for double-sided linear induction motor with short secondary*". They presented a method for calculating the performance of DLIM with short secondary by deducing the analytical solution of the air gap flux density first from 1D electromagnetic field equations, then from the equivalent circuit of the motor. This took into account both longitudinal and transverse end effects. They developed the correction coefficients for magnetizing reactance and secondary resistance on the basis of the equivalence principle, which says the

complex power derived from the circuit is identical to that is from the field. They calculated the main characteristics of the proposed circuit with and without end effects. They showed that the FEA matched very well with the starting performances of the circuit [31].

The paper *"Computer simulation study on optimization of linear servo motor used in CNC machines"* explained that DAPMLSM are suitable for high speed and high precision servo feedback systems used in CNC machine tools. The only problem discussed in the paper is the thrust ripple caused by non-sinusoidal magnetic field distribution. In this study, the verification method used FEA to study motor characterstics. The computer simulation results matched well with the prototype data. The paper claimed that FEA method was accurate. The main structure of DAPMLSM was analyzed by using these FE calculations. The key components were the magnet thickness which effects the amplitude and the pole-arc coefficient which effects both amplitude and its distribution. In the paper it is discussed that the distribution condition of the magnetic field in the air-gap could be improved effectively by optimal design of the pole-arc coefficient and that the thrust fluctuations could be reduced [33].

In 2010, Yu-wu Zhu and Yun-hyun Cho studied elevator systems and published "*Structure selection of permanent magnet linear synchronous motor for ropeless elevator system*". They indicated that the most important requirement is the high force density for RLES. Besides having a large detent force, iron core PMLSM is indicated as the best choice. The characteristics of the detent force, normal force and the thrust of PMLSM was investigated with different structures. As a result, the long stator double-sided slotted iron core type PMLSM with fractional slot winding was selected for the best performance after FEA [34].

*"Topology structure selection of permanent magnet linear synchronous motor for ropeless elevator system"* was published by Yu-wu Zhu, Sang-geon Lee and Yun-hyun Cho in 2010, to discuss the high force density needed to make the ropeless elevator system practical. According to the paper, for this kind of application apart from having a large detent force, the best choice of motors is PMLSM. The paper investigates different motor topology structures for PMLSM to see the characteristics of detent force, normal force and thrust. In conclusion the study suggests to use the

long stator double-sided slotted iron core type PMLSM with fractional slot winding [35].

## 3. MOTIVATION OF THE STUDY

The study started in 2014 under the lead of Assoc. Prof. Ozgur Ustun. The purpose of the thesis is to design a double-sided coreless linear motor with precise position control. High precision is very important for high speed, fast acceleration and quick settling times, all of which decrease cycle time and will increase productivity. This is the main problem in mechanical and positioning devices, if extreme accuracy or super smooth motion is of concern.

In this research, the electrical system consists of a power supply (DC voltage source that can be a battery or a secondary power supply), a power converter (in the most common case a three phase pulse width modulated inverter), an electrical motor (in this case a linear motor) and a control system that recieves signals from sensors (voltage sensors, current sensors and motor speed and position sensors) and generates control signals for inverter transistors.

The structure of the electrical sytem is presented in Figure 3.1.

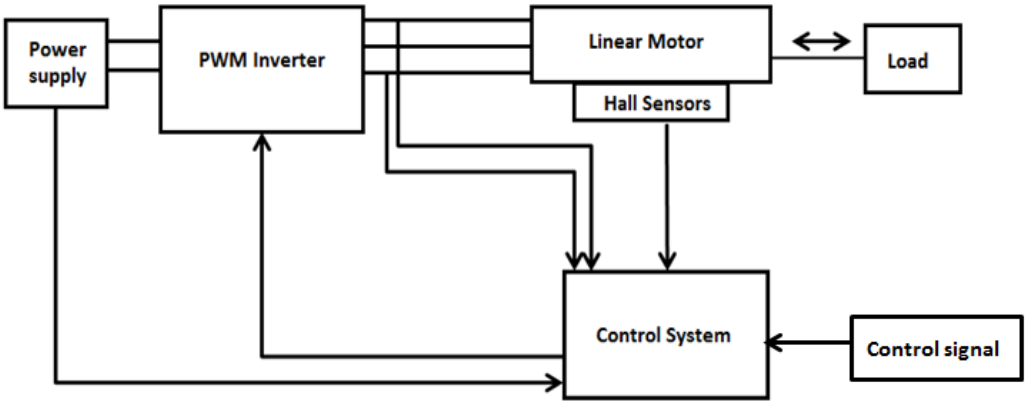


**Figure 3.1 :** The structure of linear motor electrical system.

This thesis focuses on the development and optimization of one part of the system explained above – the design of the linear motor. The design of the linear motor includes the following steps:

1) Design of the motor geometry based on given technical requirements (rated force, rated voltage and power)
2) Selection of materials
3) Validation of the design based on FEM analysis (ANSYS-Maxwell®)
4) Design optimization by taking simulation results into consideration

Power electronics and control circuit will not be discussed in depth, as the main focus of this thesis is the motor design. Motor design, analysis, production, initial testing and basic power electronic circuit are investigated. The two important focuses of the thesis are material selection and winding optimization for the needed force.

Designing a short stroke precise positioning linear motor requires special considerations. A coreless double-sided motor is designed in this work. Coreless structure provides a smooth movement. In a coreless motor, cogging force and the reluctance force occur because of the interaction between the magnets and the teeth. This becomes a problem when high precision motion control is needed. In a coreless motor, even though there is a cogging force because of the windings, this problem is negligible and can be smoothened with special winding arrangements [29]. Having double sides allows the motor to work at very high, very low speeds and to accelerate faster.

The study started based on the existing magnets NdFeB. These magnets are relatively expensive but have high performance as their efficiency and energy are higher than other type of magnets (e.g. ferrites.), although their Curie temperature is low. The needed force was 40N. As known, force depends on the magnets and the coil arrangement. A two-layered coil structure and 22 magnet pairs are used in the model. The body is made of steel material, as it is lighter and occupies less volume. This gave the basic specifications of the geometrical design. After the first decisions on the motor dimensions were taken, a simplified electromagnetic analysis is performed. For this analysis the motor drive is also taken into consideration.

Secondly, mechanical data is examined for the motor design where the mechanical equations of the motor is derived. This is followed by motor tests and comparison of the tests with electromagnetic analyses. Later on, the production phase is introduced. Finally the conclusion and the future investigations is discussed.

Some of the important specifications for the linear motor are listed in the table below:

**Table 3.1 :** Double-sided coreless linear motor data.

| **Motor Specifications** | |
|---|---|
| **Feature** | **Value** |
| **Magnets** | |
| Magnet Width | 19 mm |
| Magnet Thickness | 7 mm |
| Number of Magnets | 22 pole pairs |
| Magnet Spacing | 2.5 mm |
| **Coils** | |
| Coil Width | 14 mm |
| Coil Thickness | 8.5 mm |
| Number of Coils | 6 |
| **Yoke** | |
| Total Lentgh | 490.5 mm |
| Effective Length | 170 mm |
| Yoke Thickness | 5 mm |
| **General Specifications** | |
| Configuration | 6 coil/8 magnet |
| Model Depth | 57 mm |
| Total Weight | 10.5 kg |
| Hall Sensors | 3 |

In the table, “effective length” is defined as, the length of the motor that is covered by magnets which faces the coils. In total, there are 22 pole pairs. In the FEA model only 8 pole pairs is modeled because of the periodicity of the magnetic field. Hall sensors that are mounted on the real motor are not included in the FEA model.

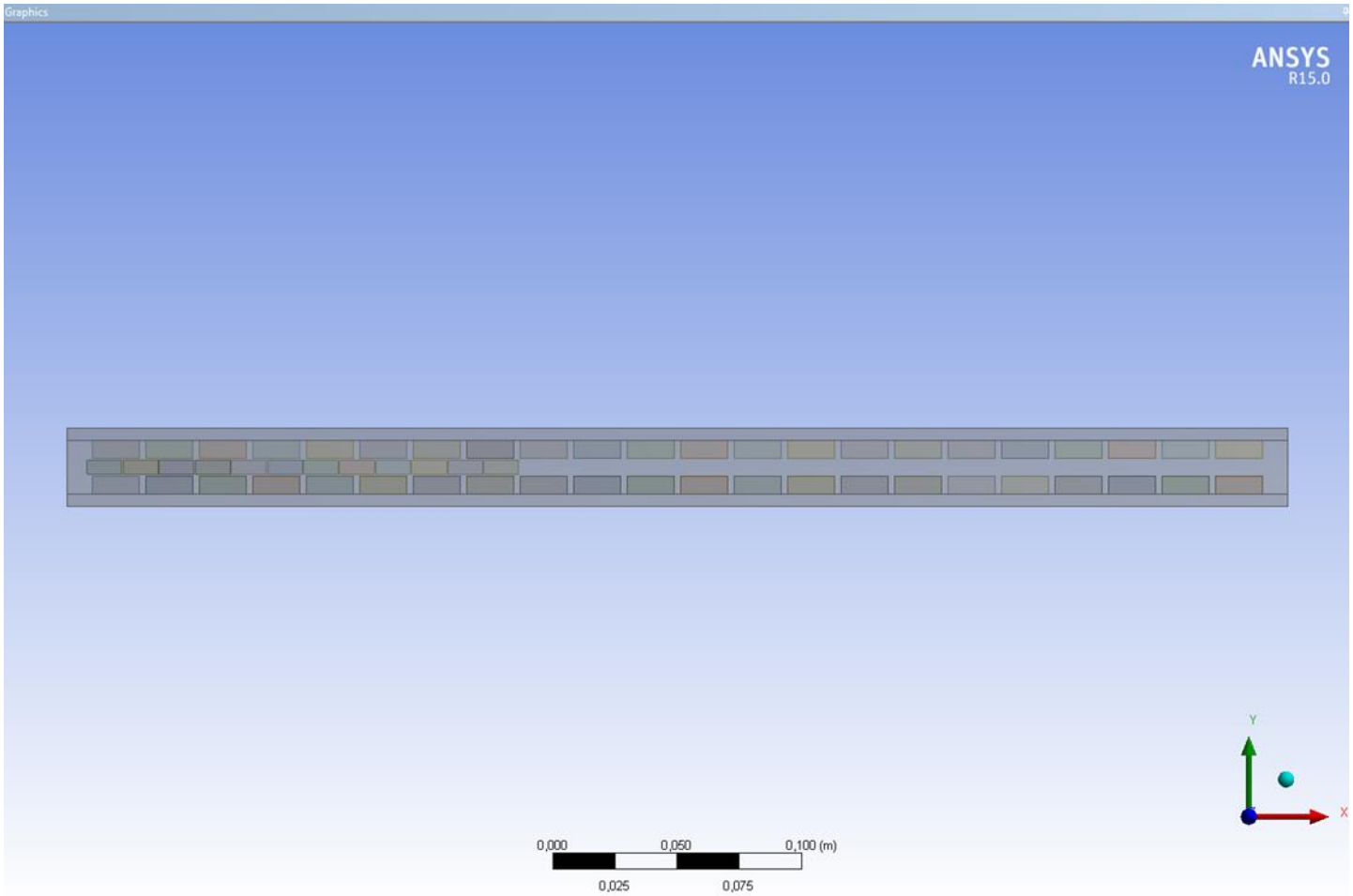


**Figure 3.2 :** Linear motor CAD drawing from the top.

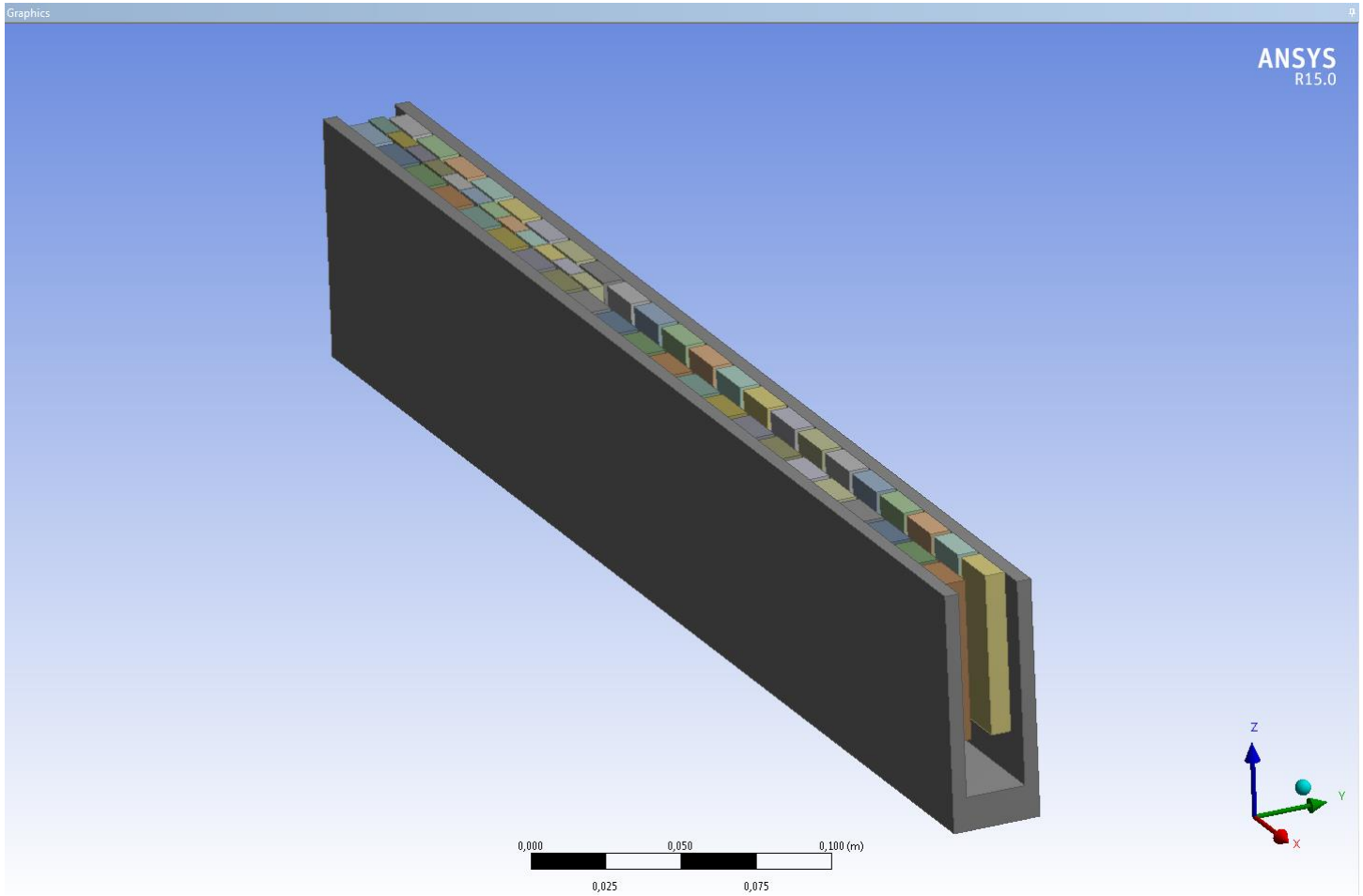


**Figure 3.3 :** Isometric view of the linear motor without end-turns.

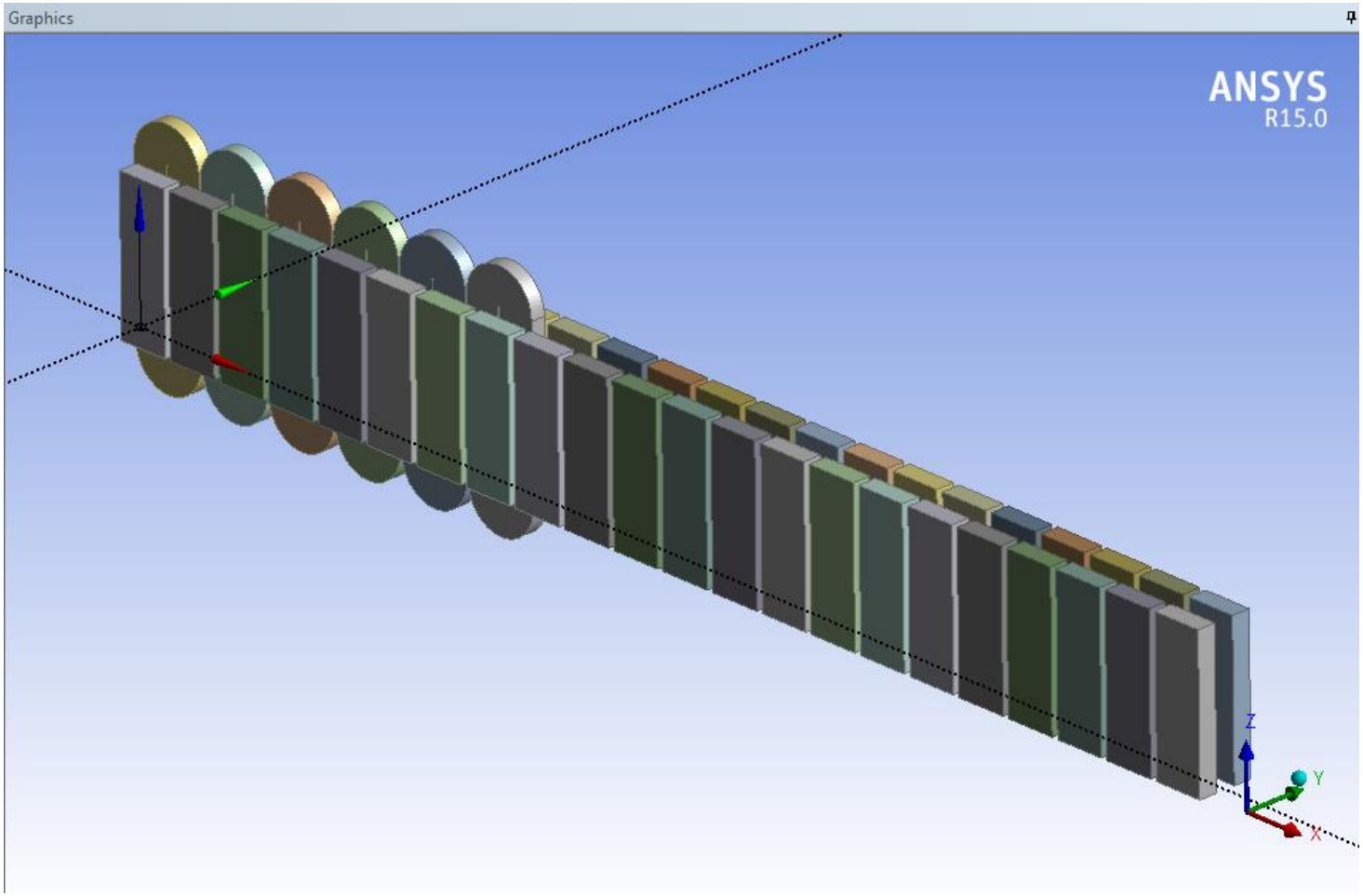


**Figure 3.4 :** Isometric view of magnets and coils with end-turns.

# 4. MAGNETIC ANALYSIS OF THE MOTOR

A motor is normally designed based on the needed output that the user is looking for. This criterion must be met. In the design of a motor, the designer should consider magnetic flux in all type of electrical machines (e.g., generators, motors and transformers), as the main component of energy conversion is the magnetic flux. When looking at the production of the magnetic flux, the designer should see that it all depends on the field or magnetizing winding of the moving parts. The major considerations to evolve a good design are cost, durability and compliance with performance critera as laid down in specfications.

## 4.1 Electrical Motors

An electrical machine is a device that converts electromechanical energy. Electrical motors are essentially inverse generators where a current through coils of wire causes some mechanical device to rotate. The core underlying principle of motors is electromagnetic induction. A motor is basically a generator run backwards that uses current to produce motion as opposed to using motion to produce current.

Like generators, electric motors consist of a stator, a rotor, electric current, magnetic fields and a rotating field. They can be classified as DC motors, AC motors and other special types of motors (e.g., stepper motors, hysteresis motors, reluctance motors etc.). In an AC motor, AC current flows into the coils and creates a rotating magnetic field where in a DC motor magnetic field is created directly.

The energy equations of a motor can be found below. The input and output power are expected to be equal in all conditions (4.1), where the input power is the product of voltage (E) and current (I) and the output power is the product of force (F) and velocity (v).

$$P_{in} = P_{out} \tag{4.1}$$

$$P_{in} = E \cdot i \tag{4.2}$$

$$P_{out} = F \cdot v \tag{4.3}$$

The linear motor that is designed in this work behaves like BLDC motors.

### 4.1.1 Linear Motors

A linear motor has almost the same principles as a rotational motor. Like all other electrical motors a linear motor has a stationary and a moving part. Linear motors can be thought as unwrapping a rotational motors. Angular dimensions and displacement are replaced by their counter parts, torque is replaced by force and the commutation cycle is the distance between two consecutive pole pairs instead of 360 degrees. The moving part is called forcer instead of rotor where the windings are placed that provide current. The magnet rail holds the rare earth magnets, providing flux by alternating polarity.

The main working principle is similar to the operation of a conventional DC rotary motor. The flux is obtained by the windings consisting of insulated copper wires on laminated cores or in existance of permanent magnets, permanent magnets provide the field flux [1]. The main goal of a linear motor is to generate force (F) by interaction of the current (I) with the flux density (B). This is demonstrated by one of the basic laws of electromagnetism named as the Biot-Savart Law, which says that if a current carrying conductor is placed in a magnetic field that is perpendicular to the current direction, a mechanical force is exerted on the conductor perpendicular to the both current and the magnetic field. This force is given by the formula:

$$\hat{F} = I \cdot (\hat{L} \times \hat{B}) \tag{4.4}$$

The equation can also be written as;

$$F = \phi \cdot n \cdot I_a \tag{4.5}$$

Here, $\varphi$ is the flux (Webers) that enters the armature from the pole face. $I_a$ is the armature current (Amperes) and $n$ is the number of conductors per meter length of the armature [1].

This is also demonstrated by the formula:

$$F = k \cdot \phi \cdot i_a \tag{4.6}$$

where k is the ratio of the conductor (copper) diameter to the overall wire diameter and known as the winding factor.

At any particular moment only one section of the armature winding is energized. This is different than the length of the magnet. If this was not the case, forces would be developed in opposite directions and the motor would stall [1].

Another important formula of a linear motor is the voltage induction formula below:

$$E = B \cdot l \cdot \nu \tag{4.7}$$

If a long conductor of length *l* is moved in a magnetic field of flux density *B* with a velocity of *v*, a voltage (E) is induced in the conductor, where *B, l* and *v* are vectors and perpendicular to each other. The equation can also be written as in (4.8).

$$E_a = k \cdot \phi \cdot \nu \tag{4.8}$$

The magnets are playing a big role in the design. Magnets are as in all other electromagnetic devices, operate in the second quadrant of the B-H curve. If a magnet having a high energy product is chosen, higher force will be derived form the equation depending on the virtual force calculation.

#### 4.1.1.1 Double - Sided Coreless Linear Motor

There are many types of linear motors. This thesis only pertains to the double-sided coreless linear motor. If a circular stator is cut into two sections and flattened, the motor becomes a linear motor. In a single-sided linear motor the force between stator and armature is perpendicular to the direction of movement. This force either attracts or repells the stator and armature. For a double-sided linear motor these forces cancel out. Since there are no iron parts on the forcer, there is no attraction between the forcer and the rails. This means there is no extra load on bearings. This helps to control the motor better and provides a better stepping. This motor type is useful for high speed control applications. Lack of friction is an advantage but there is air bearing. The disadvantages of this type of motors are the heat control and its relative

size. They are especially applicable to propulsion of belt conveyors. The picture below demonstrates the structure of the motor that is of concern in this study.

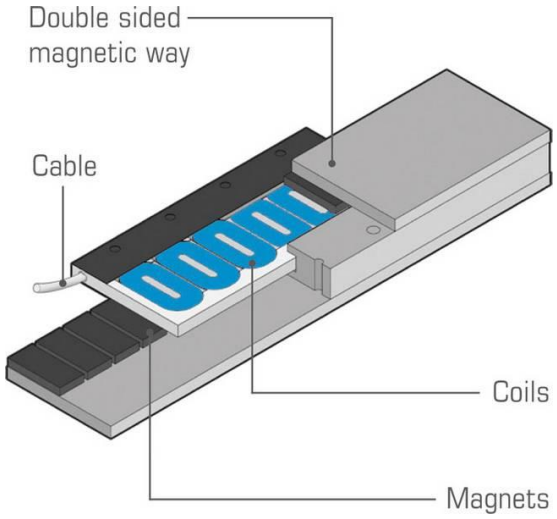


**Figure 4.1 :** Double-sided linear motor [45].

#### 4.1.1.2 Material Choice and Magnets

The most important part of the material choice when designing PM motor is the magnets. In this section, the concentration is on the properties of the magnets.

There are many different types of permanent magnet motors. They are classified according to diferent considerations such as field systems. The structure of a field system is closely related to the behavior of the permanent magnet that is used in the motor [16].

A permanent magnet designer should take good care of the energy product, which is the absolute value of the product of the flux density B and the field intensity H at each point along the demagnetization curve, knowing that the demagnetization curve is the second quadrant of a hysteresis curve [16].

In this project, rare earth magnets are used. These magnets have both high remanence and high coercive force, however their initial cost is high. As they have a high coercive force they can be magnetized widthwise. Since they are expensive, they intend to be produced relatively thinner. Having the same area, rare earth magnets provide twice flux density as ferrite magnets because of their high remanence [16].

**Table 4.1 :** NdFe35 magnet material properties.

| Parameter | Value |
|---|---|
| Relative Permeability (Simple) | 1.0997785406 |
| Bulk Conductivity (Siemens/m) | 625000 |
| Coercivity (A/m) | -890000 |
| Mass Density (kg/m$^3$) | 7400 |
| Remanence | 1.23T |

The next important material choice is the material for stator back iron. The material used in this research is a steel alloy having the properties in the table and the BH curve in figure below.

**Table 4.2 :** Steel_1010 material properties.

| Parameter | Value |
|---|---|
| Relative Permeability (Non-linear) | BH Curve |
| Bulk Conductivity (Siemens/m) | 2000000 |
| Mass Density (kg/m$^3$) | 7872 |

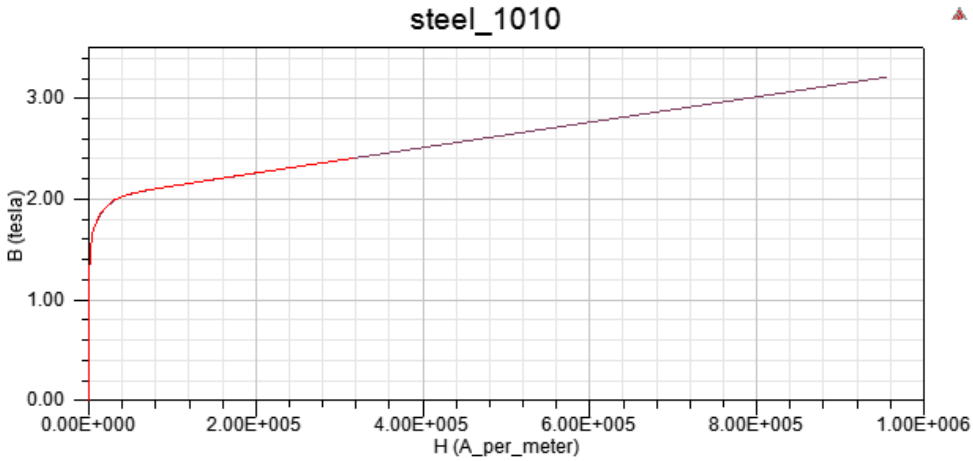


**Figure 4.2 :** BH curve of the steel material.

As seen from the BH curve above, this kind of steel saturates around 2T [36].

### 4.2 Designing a Linear Electrical Machine

The basic design of an electrical machine involves the dimensioning of the magnetic circuit, electrical circuit, insulation system etc., by applying the foundational theories and principles of electromagnetism like, Faraday's Law, Lenz's Law, Biot-Savart Law along with Maxwell's equations.

Typically there are more than one solution for the confronted problems. The most suitable design would be the one ensuring the product performing in accordance to the requirements at higher efficiency, lower weight of material for the desired output,

lower temperature rise, lower cost as well as being reliable and durable. It is expected that the design can be adapted to the requirements and specifications and finds a compromise between the ideal design and a design which complies with manufactring conditions.

An electrical machine design involves a number of assumptions and constraints, where the final design values are generally obtained by using iterative methods. Many designers use software to optimize their designs. By using FEM, the effect of a single parameter on the dynamical performance of the machine is studied. It is also possible to perform some tests which are not even feasible in laboratory setup, as they can be performed virtually by FEM.

There are several factors to consider in electrical machine design. As stated above, the basic components of all electromagnetic apparati are the field armature windings. Therefore, designer should pay attention to the following:

1) Magnetic circuit or flux path should establish the required amount of flux using minimum MMF and the core losses should be minimal

2) Electric circuit and windings should ensure required EMF that is induced with no complexity in winding arrangement and the copper losses should be minimal

3) Insulation should ensure trouble free separation of machine parts and should confine the current in the prescribed paths

4) Machine parts should be robust

The art of successful design lies not only in resolving the conflict for space between iron, copper, insulation and coolant but also in optimization of cost of manufacturing, operating and maintanance charges.

There are also some limitations of the design coming from material properties and others such as cooling, etc. The limitations stem from saturation of iron, current density in conductors, temperature, insulation, mechanical properties, efficiency and power factor. Taking saturation into account, higher flux density reduces the volume of iron but drives the iron to operate beyond the knee point of the magnetization curve. This increases the core losses, and excessive excitation is required to establish

a desired value of flux. Higher current densities reduce the effective volume of copper but increases the losses and temperature. Temperature poses a limitation on account of possible damage to insulation and other materials. Another limitation comes with the mechanical strength of the materials in the case of large and high speed machines. High effieciency and high power factor poses a limitation on account of higher capital cost, a low value of efficiency, whereas power factor results in a high maintanence cost.

In this thesis not all the factor listed above would effect the design performance of the double-sided coreless linear motor. The FEM software chosen is ANSYS Maxwell 2015®. The results are given in accordence to the calculations made by the FE simulation and discussed.

### 4.3 FEM Model and Design

FEA is widely used by engineers, scientists and researchers to solve engineering problems coming from different physical fields (as in this project it is electromagnetics). Currently FEM is known as the best technique to work on electromagnetic problems. In essence, the FEM solves any engineering problem that can be described by a finite set of spatial partial derivative equations with appropriate boundary and initial conditions. Problems can be static, steady-state or transient engineering applications coming from different markets such as automotive, aerospace, nuclear, biomedical, etc.

FEM has a solid theoretical foundation. It is based on mathematical theorems that ensure the accuracy of the calculations coming from fields towards the exact solution. For the domain solutions the spatial discretization is refined and used adapted to the estimated constants.

In Maxwell Field Solver, Maxwell's Equations are used to solve electromagnetic field problems in a finite region with appropriate boundary and initial conditions when necessary. The only finite element structure possible are the tetrahedral elements. A finite element mesh is created by the assembly of all tetrahedral elements in the model.

Maxwell has different options to solve an electromagnetic problems such as special boundary conditions or automatic mesh refinement. In some cases model is meshed

automatically by the mesher. Inside each tetrahedron, the unknown characteristics for the field being calculated are represented as polynomials of second order. Therefore, there needs to be a finer mesh in highly energized areas.

### 4.4 FEM Model Design and Specifications

The main principle of designing an electromagnetic project with a FEM tool is that the design should be as simple as possible and as complicated as necessary. As described in the previous chapters, the total motor model is 490.5 mm including 22 pole pairs opposing each other. To simplify the design, only 8 pole pairs facing the coils are modeled. This means the smallest repeated geometry in terms of electromagnetic field behaviour is modeled.

By using matching boundry option in Maxwell, periodic structures are modeled and the project is easily simplified. To assign this type of boundary condition, a master and a slave boundary are needed on both edge of the model. The boundary assignments on the edge of this linear motor model are given so, that the H field behaves the same on both sides which is described in the software as $B_s=B_m$. Here, the "*m*" and "*s*" indicators mean "master" and "slave" while "B" meaning magnetic flux density.

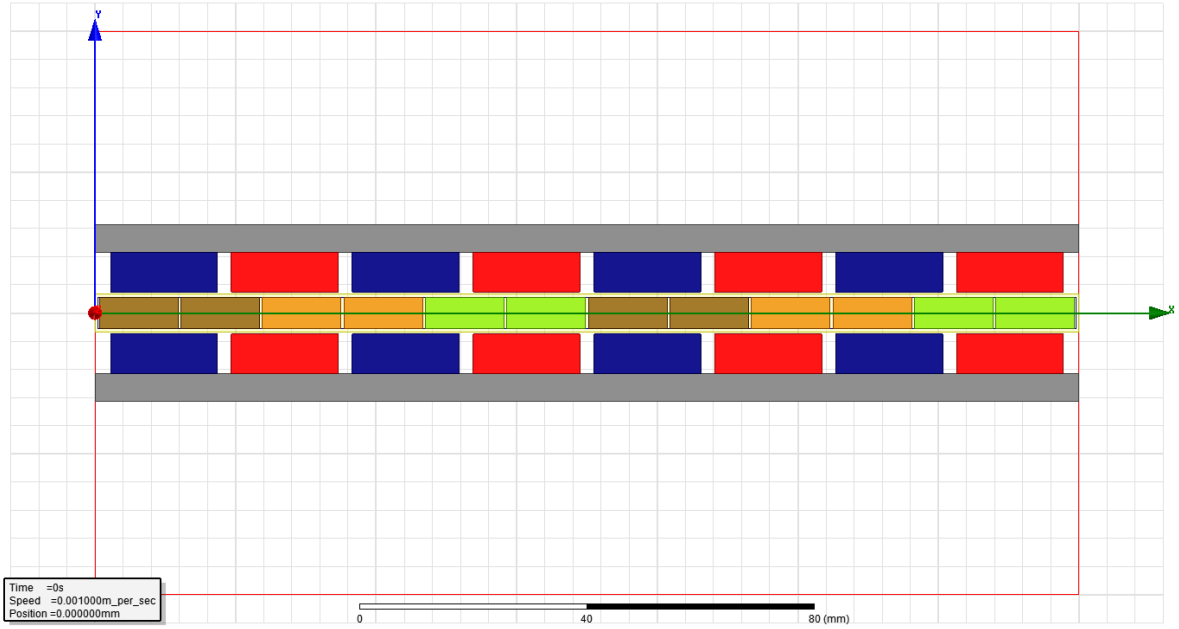


**Figure 4.3 :** Simplified FEA model of the motor.

There are 20 turns in each winding. The motor is known as 4:3 motor, meaning four magnets face three windings. In Figure 4., blue magnets are magnetized through plus y-direction and red magnets are magnetized through minus y-direction. There are two pairs of all three phases as A being brown, B being orange and C being green. A 2D simplified model of the motor is designed in Maxwell. A 2D model is not as accurate as a 3D model, however, it is a good approximation. In the 2D model of the motor, end turns of the windings are neglected.

First, 0A constant current is given to each phase to see the back-emf without excitation. Then the finite element mesh is obtained. The simulation took 4 minutes creating 16328 mesh elements. The meshed model and the back-emf plot is shown in Figure 4.4 and Figure 4.5.

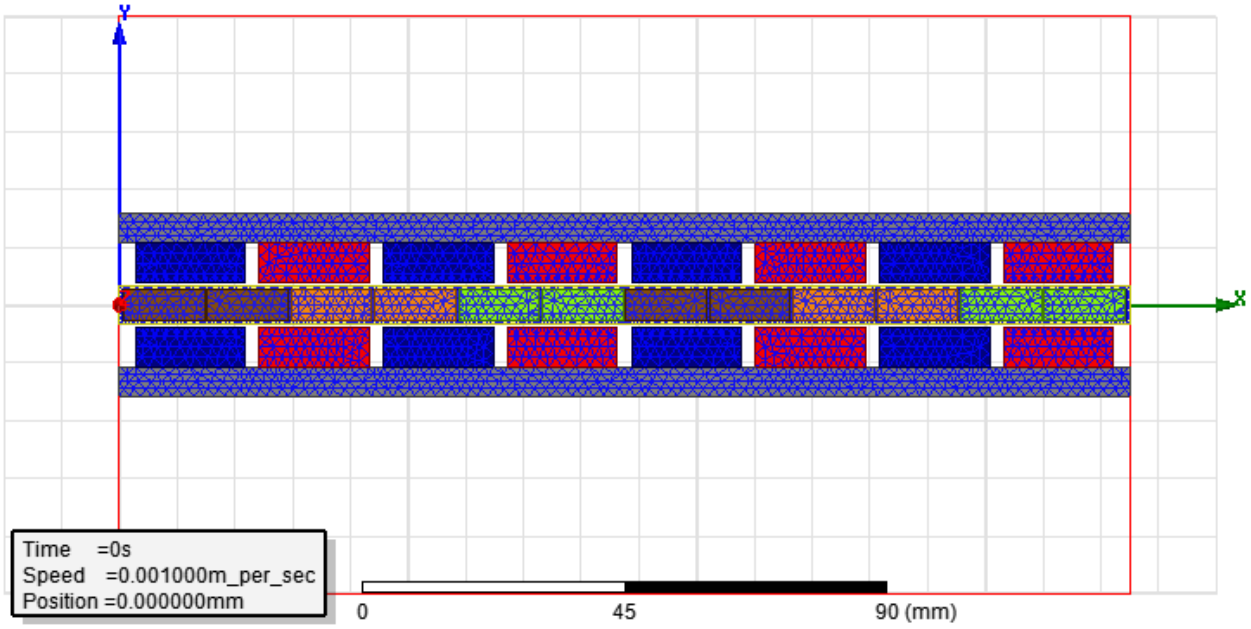


**Figure 4.4 :** Model with finite element mesh.

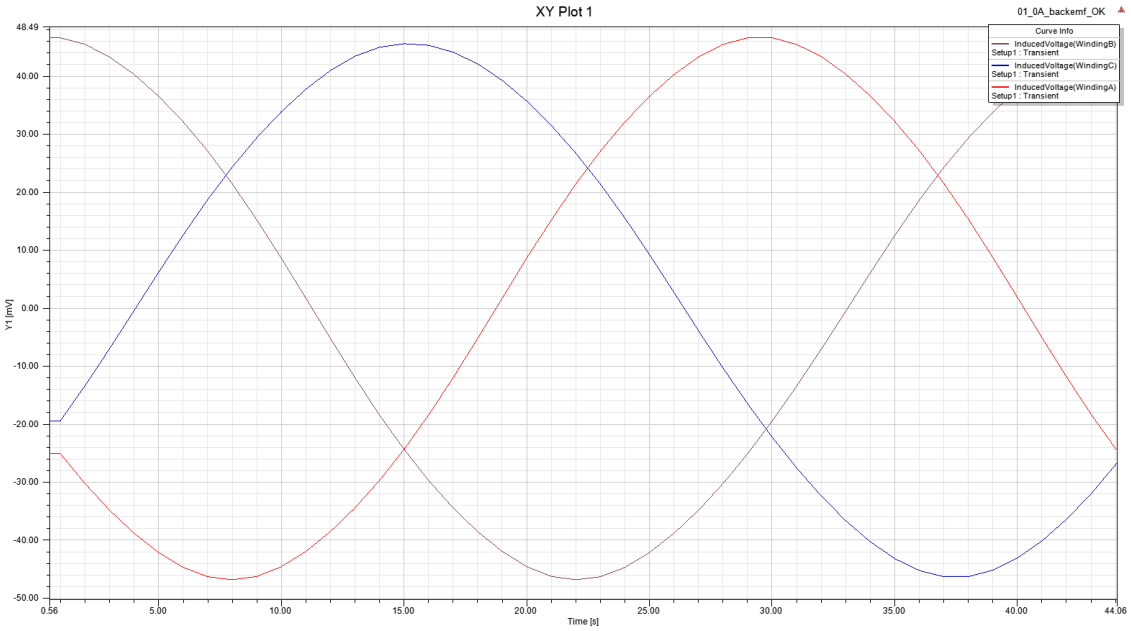


**Figure 4.5 :** Back-emf of the linear motor.

As seen from the results, this is a sinusoidal motor when no excitations applied. Its period is 44 sec and its frequency is 0.02272 Hz.

### 4.4.1 Verification of Simulation by Hand Calculation

First Faraday's law is verified by a hand calculation by using the information obtained from the model in the formula below and the value is compared with the simulation result.

$$F = B \cdot L \cdot I \tag{4.9}$$

To verify this equation motor is run in Maxwell by using 10A constant current excitation (which is the amplitude in the transient excitation) and force is calculated as 39N average from the simulation.

For the hand calculation the value of exact area of the coil below the magnet was needed. This area is calculated as 70.125 $mm^2$. Knowing that the total area of the coil having 20 turns is 77 $mm^2$ , the number of turns for 70.125 $mm^2$ area is calculated as 18.214. This infomation is due to number of turns in a coil being directly proportional to the area of the coil as they are equally distributed and the J (current density) is homogeneous accross the cross sectional area of the coil. The part of the coil that is exactly below the magnet colored in red is shown in Figure 4.6.

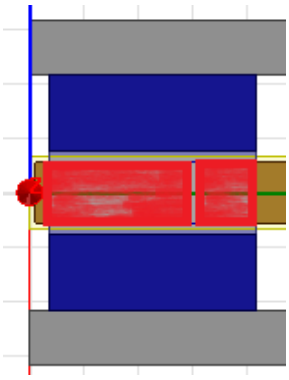

**Figure 4.6 :** The cross sectional area of the coil exactly below the magnet.

The y-component value information of B field on a magnet is also calculated by the simulation as 0.7T. This measurement is obtained on the center of any magnet in the design. It is known that the B field is not equal everywhere on the magnet but for an approximated hand calculation this information shall be acceptable.

The magnet depth is 57 mm. Placing all the information (B field value, current value and the length of the magnet)in the equation above (4.9) force is calculated as below:

$$F = 0.7 \cdot 10 \cdot 0.057 = 0.39N$$

As there are four coil-turns for the same phase (Coil-in and Coil-out will make one coil-turn and there are two coils for each phase) this force value is needed to be multiplied by 4 to get te force value for one turn.

$$F_{PhaseA-1turn} = 0.39 \cdot 4 \simeq 1.6N$$

It is approximated that the total value is almost 1.6N. Since there are 18.214 turns exaclty facing a magnet, the force for the calculated number of turns is:

$$F_{motor} = 1.6 \cdot 18.214 \simeq 29.14N$$

However, the rotating field vector is needed to be considered. In a three phase system, if the three phases have 120 degrees in between, and if it is linear, the resulting rotating field vector will be the 1.5 times of the vectors. So the total force effecting the motor is calculated as:

$$F_{motor} = 29.14 \cdot 1.5 \simeq 43N$$

After the hand calculation, the linear motor is run in the software and the force value is obtained. The force over time curve is plotted and the average value of the total force is calculated. In the simulation result below it is visible that the average force value is approximately 39N.

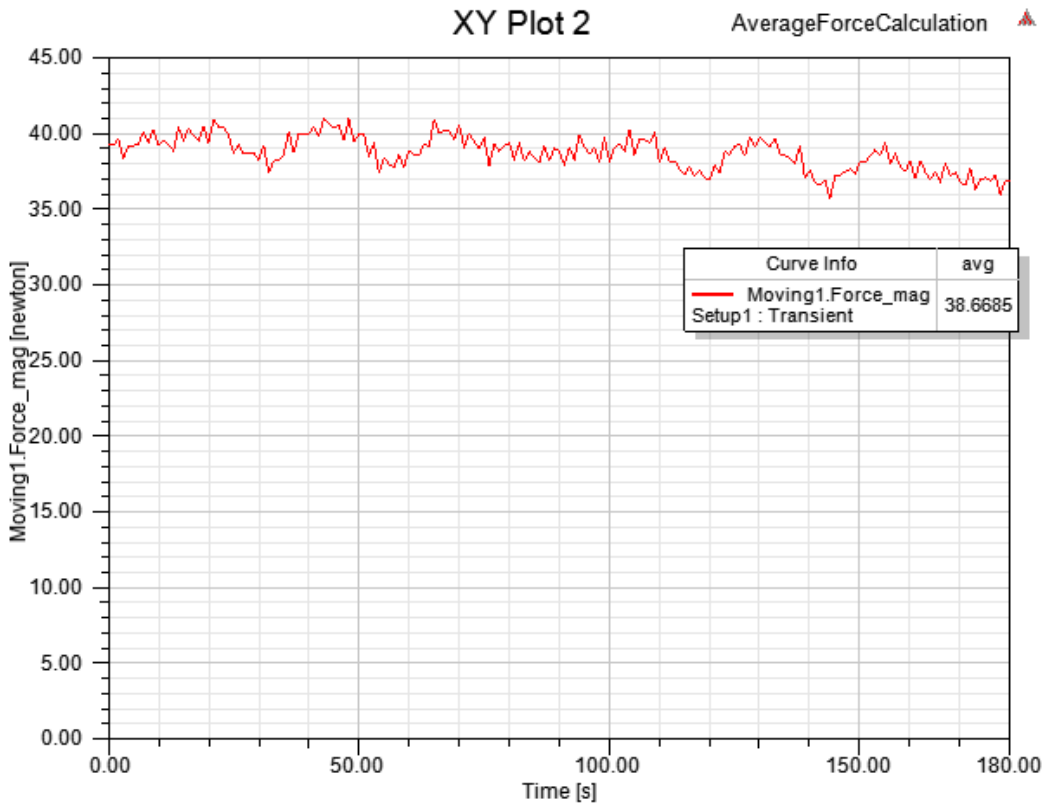


**Figure 4.7 :** Average force calculation from Maxwell simulation results.

The difference between the hand calculation and the simulation result is numeric. In Maxwell Field Solver there are several points that effects the results such as time step, non-linear residual value selection and the quality of the mesh. For that reason, the difference is negligible.

### 4.4.2 Motor Electromagnetic Design

After designing the motor in Maxwell2D the PWM circuit is created by using Maxwell Circuit Editor which is a basic complementary power electronics designer for Maxwell software. The switches are considered ideal in the inverter and only the inverter part has been taken into consideration. Motor external circuit can be seen in Figure 4.8.

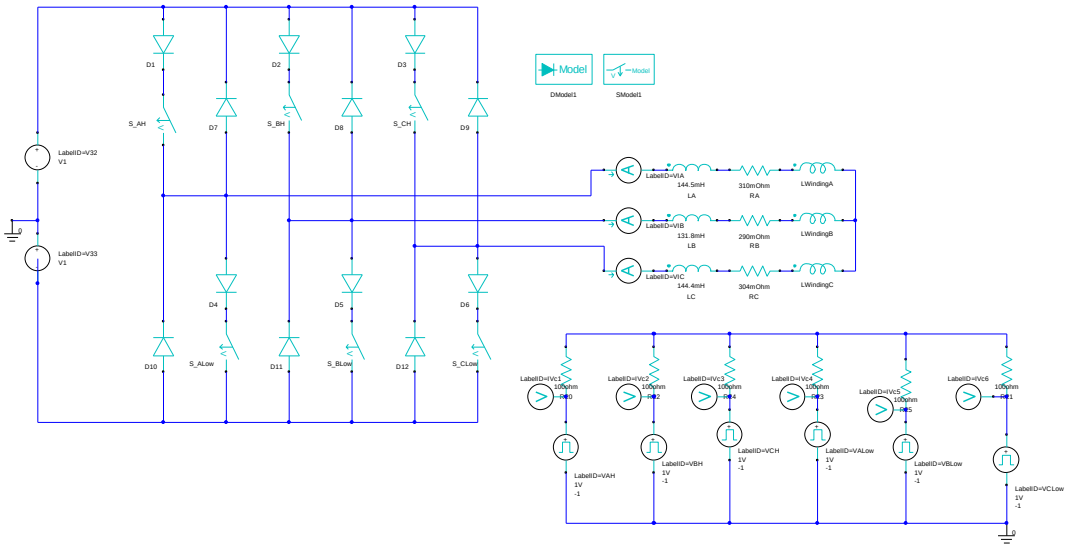

**Figure 4.8 :** Motor drive inverter circuit.

The analysis is made with a constant speed of 1mm per second. The coils are excited by using the circuit on Figure 4.8. The winding resistances and inductances are defined similar to the real values. A 3V DC voltage is applied to the inverter circuit. The period was 44s as stated before. The simulation is run for three electrical cycles, which is 132s. Time step is taken as 44/50/20s = 0.44s. The model is run in a quad cored i7 processor 16GB RAM machine and the analysis took around 2 hours. Analyses results are given in XY-Plots and as field distributions.

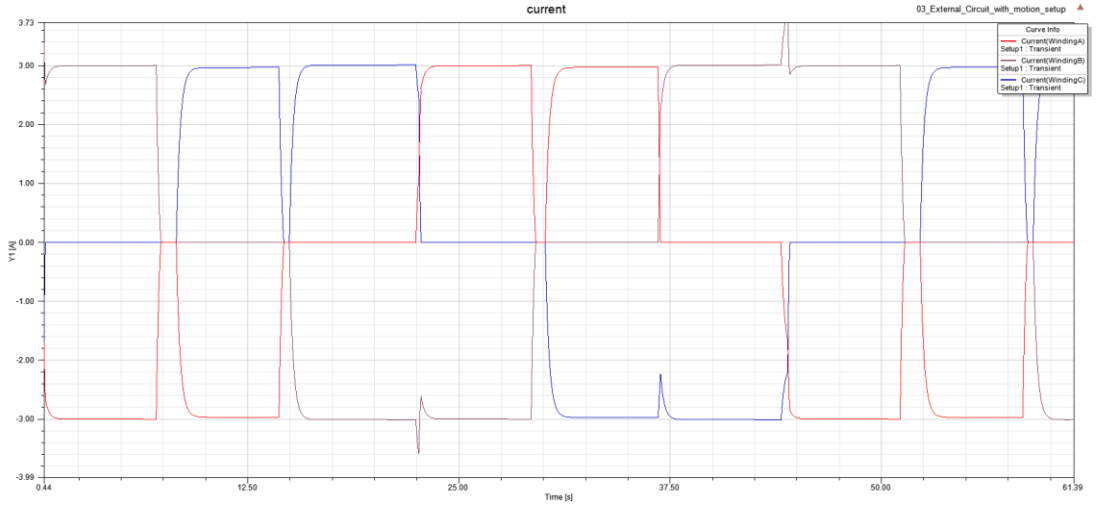


**Figure 4.9 :** Winding currents.

The spikes are occuring during the switching of the other two phases. With a more precise timing in switching this problem can be solved.

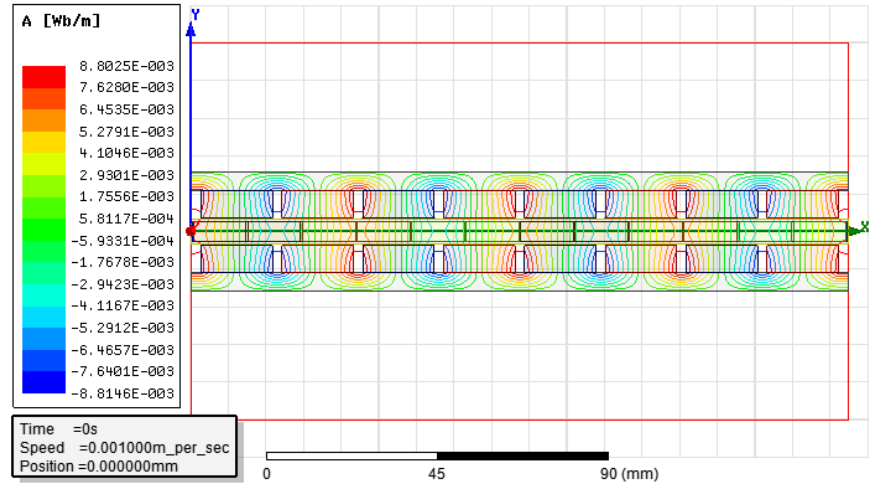


(a)

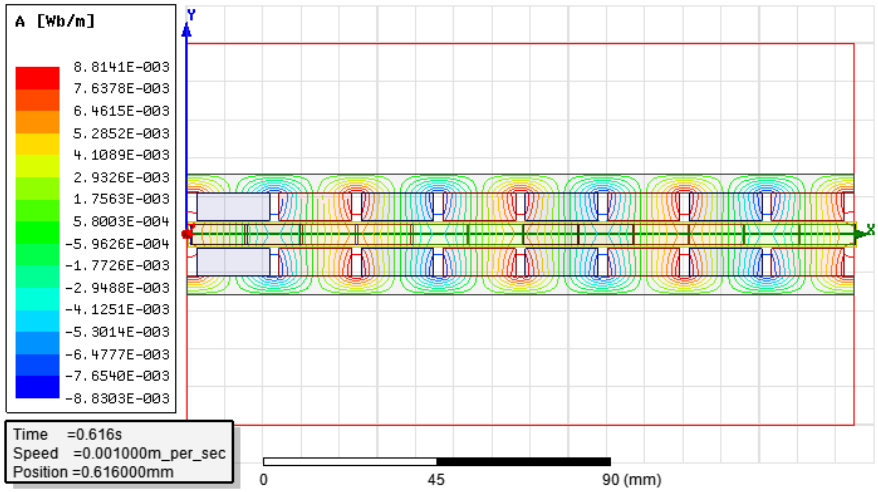


(b)

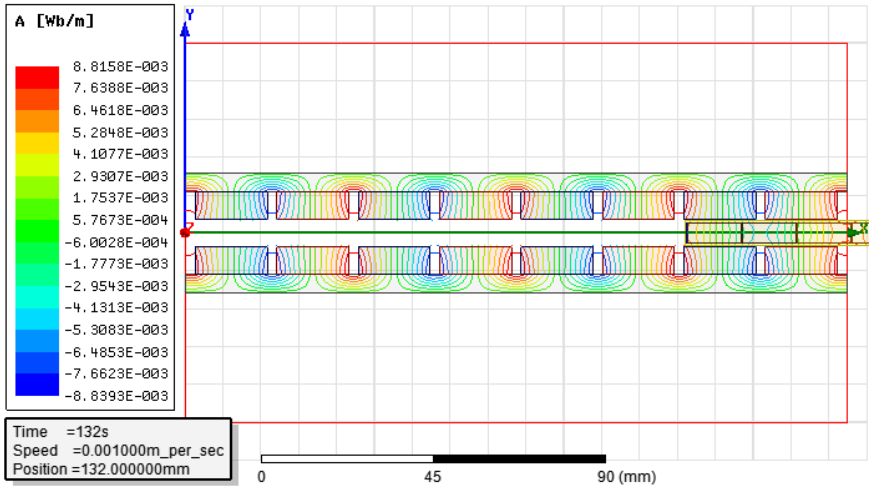


(c)

**Figure 4.10:** Flux line overlays at times a=0s, b=0.616s, c=132s and f=44s.

Flux lines for different times of movement are visible on Figure 4.10.

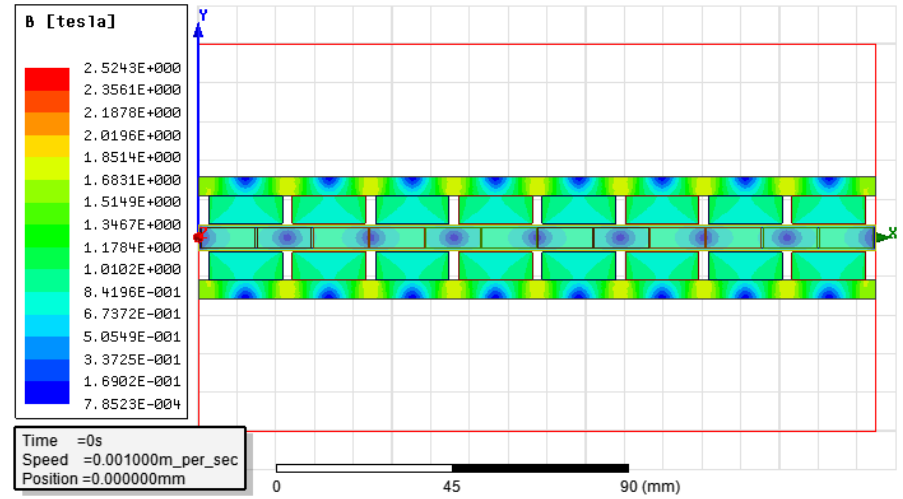


(a)

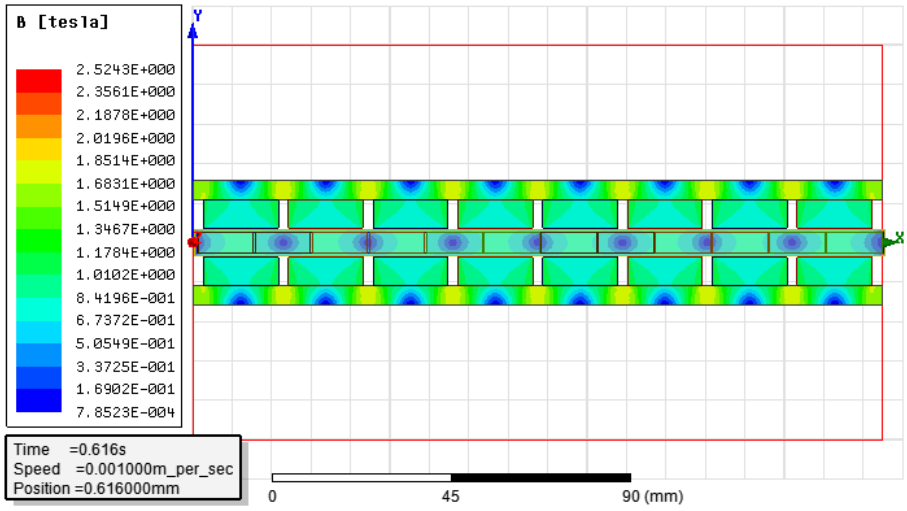


(b)

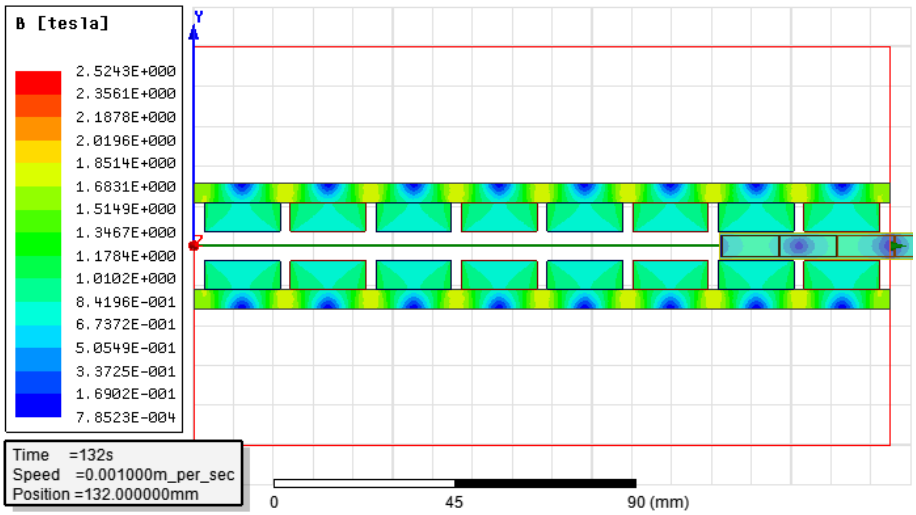


(c)

**Figure 4.11:** Magnetic field density plot at times a=0s, b=0.616s, c=132s and f=44s.

The steel saturates around 2T. In the plots, it is visible that the highest magnetic field density value is around 1.6-1.7T. 2D FEA shows that optimized motor has reasonable magnetic field density values that does not go into saturation as well as not leaving any stator back iron unused.

#### 4.4.2.1 Motor Force Calculations with FEM Design

In this chapter, motor force calculations are placed for different current values to compare the values later on with the test results. FEA is set up in transient solver where the coils are excited by three phase sinusoidal voltages. A parametric simulation is set where the current values are swept between 10A to 20A with 1A steps. After plotting the parametric set up for different current values, maximum values of the forces in x direction is calculated, as the maximum force occurs in x direction. The results for force over time are visible in Figure 4.12.

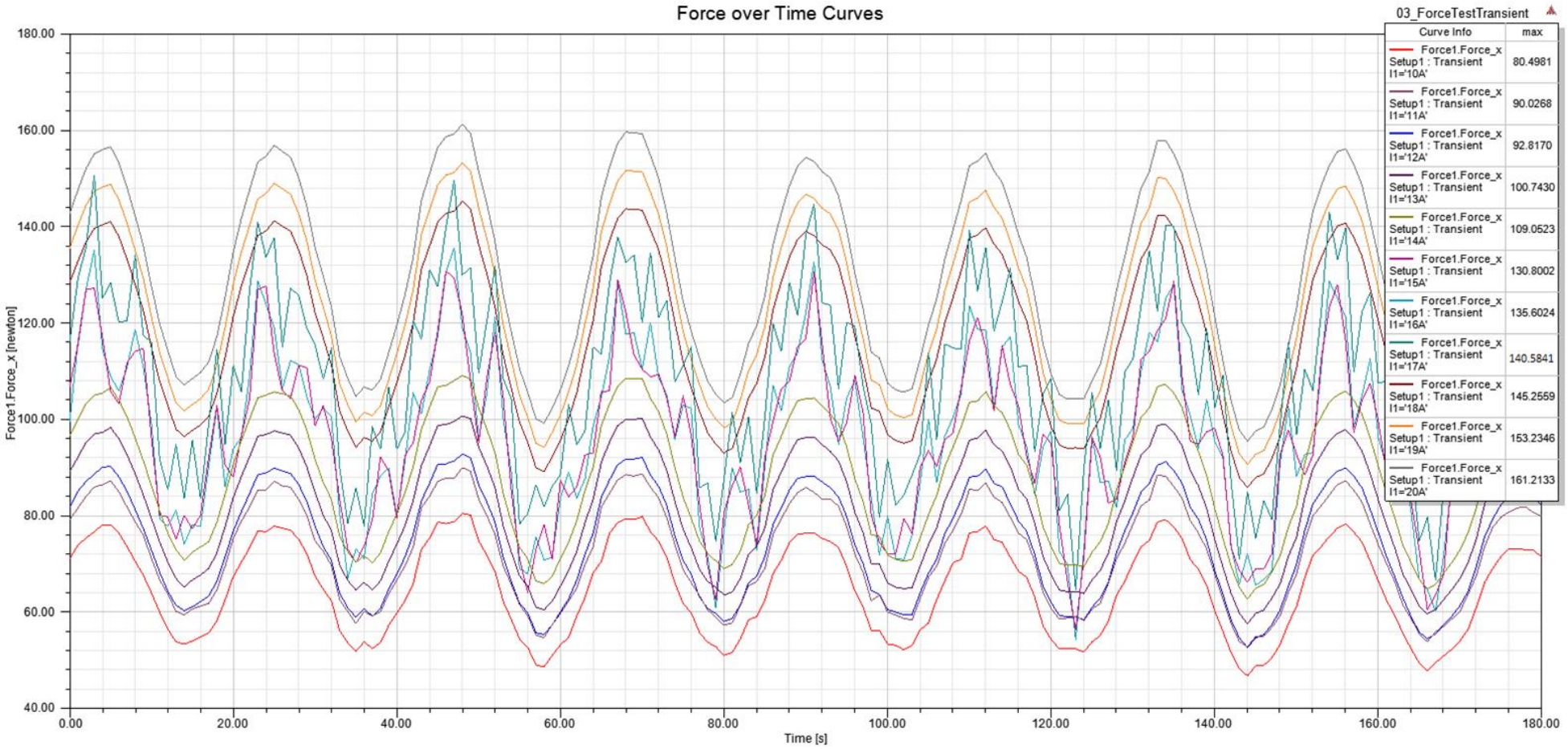


**Figure 4.12 :** Maximum values of the force for different current excitations.

FEA results are also shown below in Table 4.3.

**Table 4.3 :** Maximum force values for different current sweep results.

| Current Value [A] | Maximum Force Value [N] |
|---|---|
| 10 | 80,4981 |
| 11 | 90,0268 |
| 12 | 92,8170 |
| 13 | 100,7430 |
| 14 | 109,0523 |
| 15 | 130,8002 |
| 16 | 135,6024 |
| 17 | 140,5841 |
| 18 | 145,2559 |
| 19 | 153,2346 |
| 20 | 161,2133 |

It is expected, as the motor goes into saturation, with the current increase the difference between force values will decrease gradually. This can be seen in Table 4.3.

## 5. MECHANICAL IMPLEMENTATION OF THE LINEAR MOTOR

In this chapter the mechanical data of the motor will be investigated. First, the motor dynamics will be introduced. Based on the mechanical equations to produce the needed force, implementation details will be given. The CAD drawings and the 3D model of the linear motor will also be given.

### 5.1 State Space Model of Brushless Linear Motor

In this part of the thesis, the state space model of the linear motor is investigated. Below are the figures showing the conduction and commutation mods of the motor. It is known that in commutation all three phases are active and in conduction mode only two pahses are active.

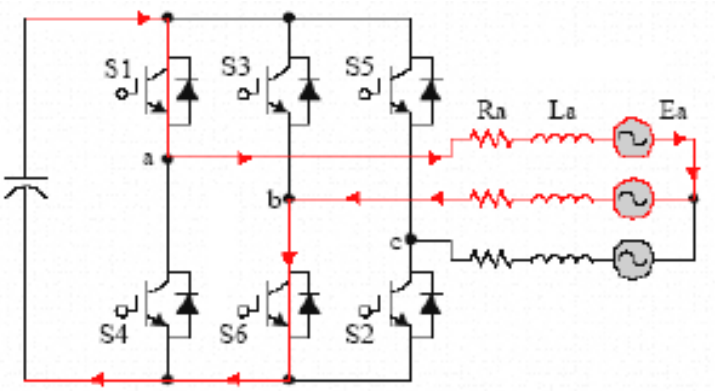


**Figure 5.1 :** Conduction.

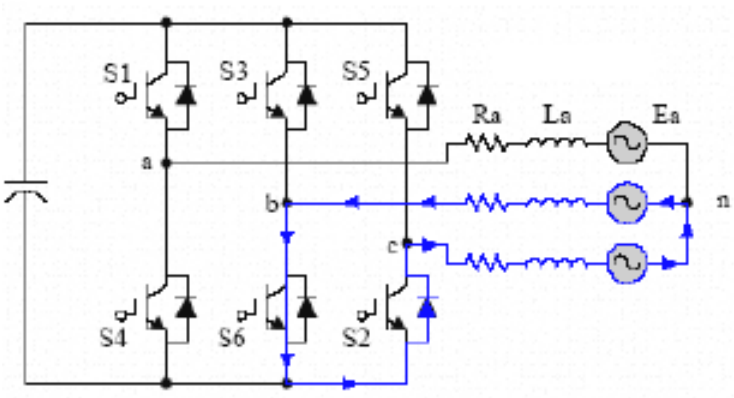


**Figure 5.2 :** Commutation.

$$i_a + i_b + i_c = 0 \tag{5.1}$$

For a time interval of $\frac{\pi}{6} < \theta e < \frac{\pi}{2}$ the system is investigated.

The sum of all currents are zero.

$$0 = R \cdot i_c + (L+M) \cdot \frac{di_c}{dt} + E_c - E_b - R \cdot i_b - (L+M) \cdot \frac{di_b}{dt} \tag{5.2}$$

$$V_d = R \cdot i_a + (L+M) \cdot \frac{di_a}{dt} + E_a - E_b - R \cdot i_b - (L+M) \cdot \frac{di_b}{dt} \tag{5.3}$$

In the equations L stands for self inductance and M stands for mutual inductance. When the equations above are placed in each other finally, the resulting equations are found as:

$$\frac{di_a}{dt} + \frac{di_b}{dt} + \frac{di_c}{dt} = 0 \tag{5.4}$$

$$\frac{di_b}{dt} = \frac{1}{3 \cdot (L+M)} \left[ -V_d - 3 \cdot R \cdot i_b + E_a + E_b - 2 \cdot E_b \right] \tag{5.5}$$

$$\frac{di_a}{dt} = \frac{1}{3 \cdot (L+M)} \left[ 2 \cdot V_d - 3 \cdot R \cdot i_a + E_b + E_c - 2 \cdot E_a \right] \tag{5.6}$$

$$\frac{di_c}{dt} = \frac{1}{3 \cdot (L+M)} \left[ -V_d - 3 \cdot R \cdot i_c + E_a + E_b - 2 \cdot E_c \right] \tag{5.7}$$

Finally the derivative equation of phase C is obtained. For this time interval the commutation equations are given in equations 5.5, 5.6 and 5.7. When the current on phase C is 0A the circuit in Figure 5. will be valid and the current equation will be:

$$i_a + i_b = 0 \tag{5.8}$$

This will lead to the formulas of conduction state seen below:

$$\frac{di_b}{dt} = \frac{1}{2 \cdot (L+M)} \cdot \left[ -V_d - 2 \cdot R \cdot i_b + E_a - E_b \right] \quad \textbf{(5.9)}$$

$$\frac{di_b}{dt} = \frac{1}{2 \cdot (L+M)} \cdot \left[ -V_d - 2 \cdot R \cdot i_b + E_a - E_b \right] \quad \textbf{(5.10)}$$

To complete the mathematical model of the motor, the equations for the mechanical side shall also be concluded. Below is the state space model of brushless linear DC motor describing the motor dynamics. The formula is similar to a rotational motor equation. The dynamics of a rotational motor can be written in the following way:

$$T_m = J \frac{d\omega}{dt} + B\omega + T_{Load} \quad \textbf{(5.11)}$$

Modifying the equation *(knowing that T=F x r)* by excluding one dimension *(r)*, the new equation can be obtained and fed to the linear motor. The formulas can be found below:

$$F_m = m \cdot \frac{dv}{dt} + B \cdot v + F_{Load} \quad \textbf{(5.12)}$$

$$\hat{F_m}(s) = s \cdot m \cdot \hat{v}(s) + B\hat{v}(s) + \hat{F_{Load}}(s) \quad \textbf{(5.13)}$$

Equation 5.13 describes the motor dynamics in the frequency domain, where $F_m$, $F_{Load}$ and $v$ describe the Laplace transform of $F_m$ and v respectively.

The dynamic equation states that the force acting on the moving unit includes an effect due to mass, a frictional component and a force corresponding to a mechanical load driven by the motor ($F_{Load}$).

The instantaneous value of the force in a brushless linear motor is written as the following:

$$F_m = k_a \cdot i_a + k_b \cdot i_b + k_c \cdot i_c \quad \textbf{(5.14)}$$

For different time intervals, same equations can be obtained similarly, for example for the second feeding step for the time interval $\frac{\pi}{2} < \theta e < \frac{5\pi}{6}$ considering the conduction mod of the motor:

$$i_b = 0 \tag{5.15}$$

$$\frac{di_a}{dt} = \frac{1}{2 \cdot (L+M)} \cdot \left[ V_d - 2 \cdot R \cdot i_a + v \cdot (k_c - k_a) \right] \tag{5.16}$$

$$\frac{di_c}{dt} = \frac{1}{2 \cdot (L+M)} \cdot \left[ -V_d - 2 \cdot R \cdot i_c + v \cdot (k_a - k_c) \right] \tag{5.17}$$

$$\frac{dv}{dt} = \frac{1}{m} \cdot \left[ k_a \cdot i_a + k_c \cdot i_c - F_{Load} \right] \tag{5.18}$$

To describe the state space model of the whole system, the induced voltage in each phase needs to be defined for all time intervals. The equations can be found below for each phase.

The motor constant change for phase A:

$$0 < \theta_e < \alpha \qquad k_a = \frac{k \cdot \theta_e}{\alpha} \tag{5.19}$$

$$0 < \theta_e < (\alpha + \beta) \qquad k_a = k \tag{5.20}$$

$$(\alpha + \beta) < \theta_e < (\pi + \alpha) \qquad k_a = \frac{-k \cdot (\theta_e - \pi)}{\alpha} \tag{5.21}$$

$$(\pi + \alpha) < \theta_e < (\pi + \alpha + \beta) \qquad k_a = k \tag{5.22}$$

$$(\pi + \alpha + \beta) < \theta_e < 2\pi \qquad k_a = \frac{k \cdot (\theta_e - 2\pi)}{\alpha} \tag{5.23}$$

The motor constant change for phase B:

$$0 < \theta_e < \left( \frac{2\pi}{3} - \alpha \right) \qquad k_b = -k \tag{5.24}$$

$$\left( \frac{2\pi}{3} - \alpha \right) < \theta_e < \left( \frac{5\pi}{3} - \alpha - \beta \right) \qquad k_b = \frac{k \cdot \left( \theta_e - \frac{2\pi}{3} \right)}{\alpha} \tag{5.25}$$

$$\left(\frac{5\pi}{3}-\alpha-\beta\right)<\theta_e<\left(\frac{5\pi}{3}-\alpha\right) \qquad k_b = k \qquad \textbf{(5.26)}$$

$$\left(\frac{5\pi}{3}-\alpha\right)<\theta_e<\left(\frac{8\pi}{3}-\alpha-\beta\right) \qquad k_b = \frac{-k\cdot\left(\theta_e-\frac{5\pi}{3}\right)}{\alpha} \qquad \textbf{(5.27)}$$

$$\left(\frac{8\pi}{3}-\alpha-\beta\right)<\theta_e<2\pi \qquad k_b = -k \qquad \textbf{(5.28)}$$

The motor constant change for phase C

$$0<\theta_e<\left(\frac{\pi}{3}-\alpha\right) \qquad k_c = k \qquad \textbf{(5.29)}$$

$$\left(\frac{\pi}{3}-\alpha\right)<\theta_e<\left(\frac{4\pi}{3}-\alpha-\beta\right) \qquad k_c = \frac{-k\cdot\left(\theta_e-\frac{\pi}{3}\right)}{\alpha} \qquad \textbf{(5.30)}$$

$$\left(\frac{4\pi}{3}-\alpha-\beta\right)<\theta_e<\left(\frac{4\pi}{3}-\alpha\right) \qquad k_c = -k \qquad \textbf{(5.31)}$$

$$\left(\frac{4\pi}{3}-\alpha\right)<\theta_e<\left(\frac{7\pi}{3}-\alpha-\beta\right) \qquad k_c = \frac{k\cdot\left(\theta_e-\frac{4\pi}{3}\right)}{\alpha} \qquad \textbf{(5.32)}$$

$$\left(\frac{7\pi}{3}-\alpha-\beta\right)<\theta_e<2\pi \qquad k_c = -k \qquad \textbf{(5.33)}$$

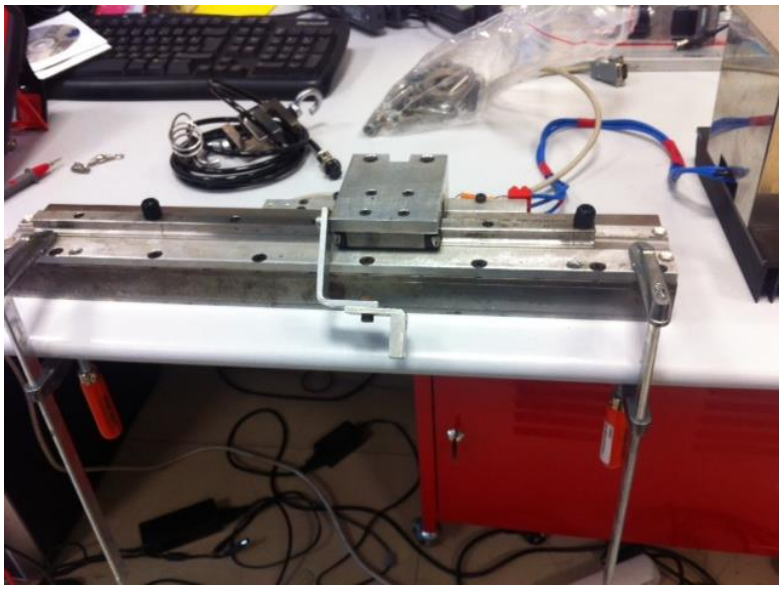

**Figure 5.3 :** Double-sided coreless linear motor.

## 5.2 CAD Drawings

A 3D drawing of the motor is created and the design details of the motor are made by using a CAD program. Once the calculations and drawing of the motor were completed, the motor size has been selected and this led to the production process. Magnets and coils were placed on the motor considering the required magnetic field distribution. The motor is first designed in 2D and subsequently the third dimension is added to create the 3D CAD drawing. However, for the electromagnetic calculations only the periodic model is simulated. The periodic model included eight magnet pairs and six coils.

## 5.3 Producing Linear Motor

The Linear motor is a 4:3 motor, meaning four magnets face three windings. As described in the previous chapter NdFeB magnets are used and stator back iron is made of steel. The linear motor does not include a housing or bearings. A 3D CAD

drawing of the coreless double-sided linear motor is shown in Figure 5.4

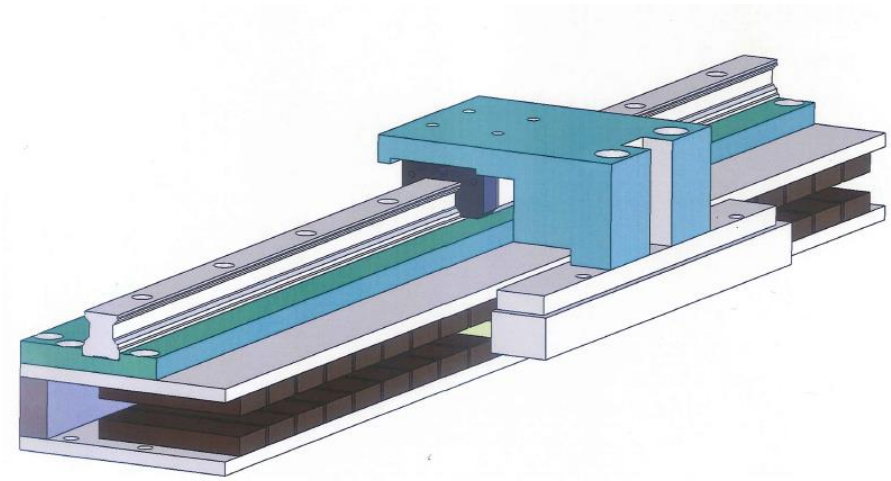

**Figure 5.4 :** 3D CAD drawing of the model.

The CAD Design was the last technical drawing prepared in the process. The production of the back iron was made on a bench and the steel was cut with a laser machine. The components of the linear motor are cut by using different CNC machines and a wire erosion machine. The stator back iron was needed to mount the magnets on. To produce the stator back iron, a steel beam was cut with a wire erosion machine using the given dimensions. After producing the stator back iron, the magnet mounting process has begun. Magnets are purchased from a company in UK (Arnold Magnet) that has the production in China. The length of the magnets are 57mm and were mounted on the stator back iron with a space of 2.5mm in between.

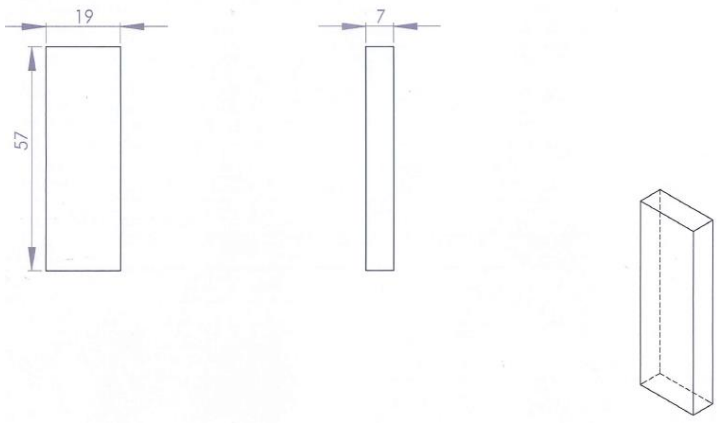


**Figure 5.5 :** Magnet details.

Magnet details are shown in Figure 5.5. first, the magnets were separated into two groups as S and N poles. By using a dogwrench, they had been attached to the stator

back iron. They were mounted on the stator back iron by using a special adhesive glue. A picture of the motor after agglutination of the magnets on the stator back iron is shown in Figure 5.6.

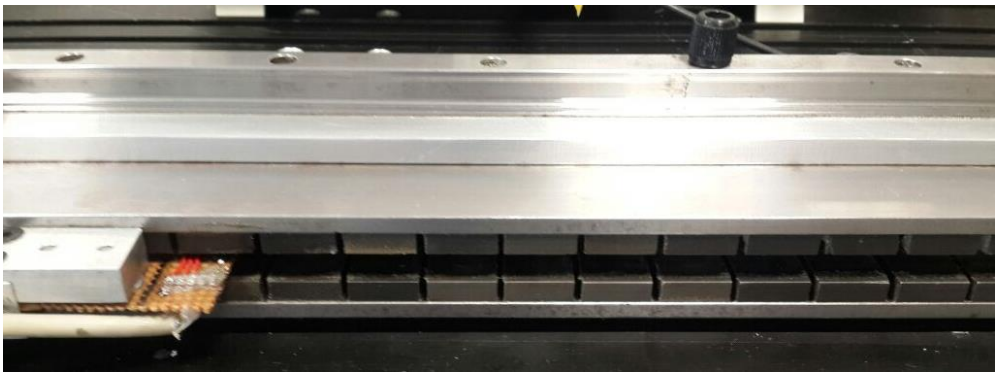

**Figure 5.6 :** Mounting magnets on stator back iron.

The coils are 5.5mm thick and 77.81mm long including end-turns.

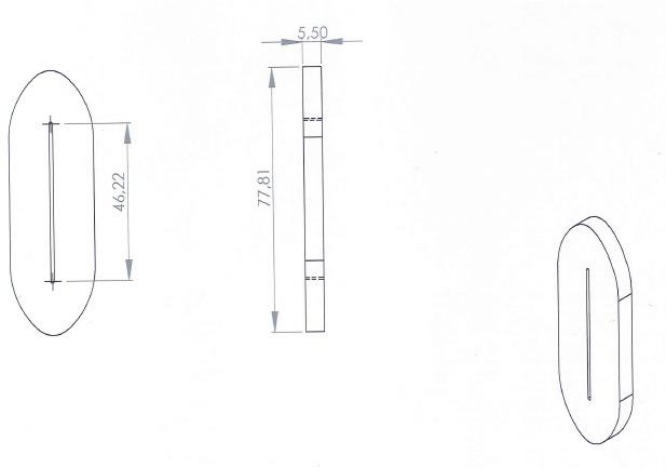


**Figure 5.7 :** Coil details.

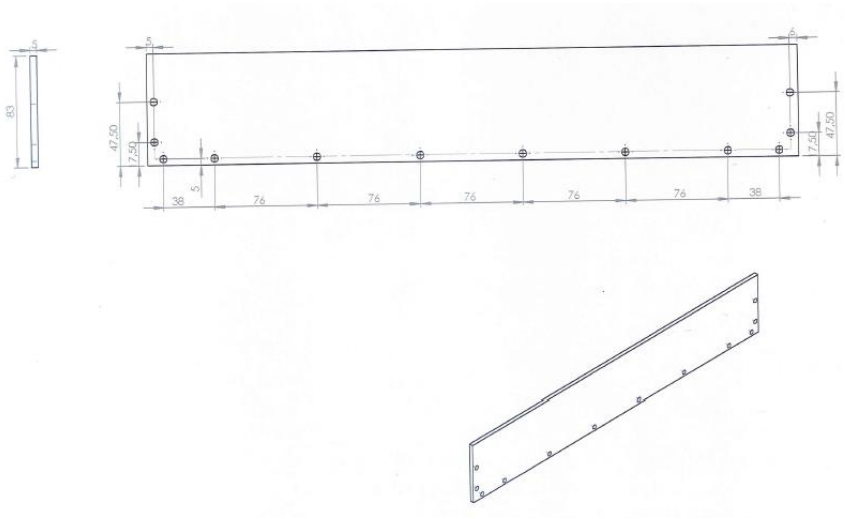

**Figure 5.8 :** Stator back iron.

There were 20 turns in each slot. The coil details are depicted in Figure 5.7 and stator back iron construction details are depicted in Figure 5.8. Winding scheme is visible in Figure 5.9.

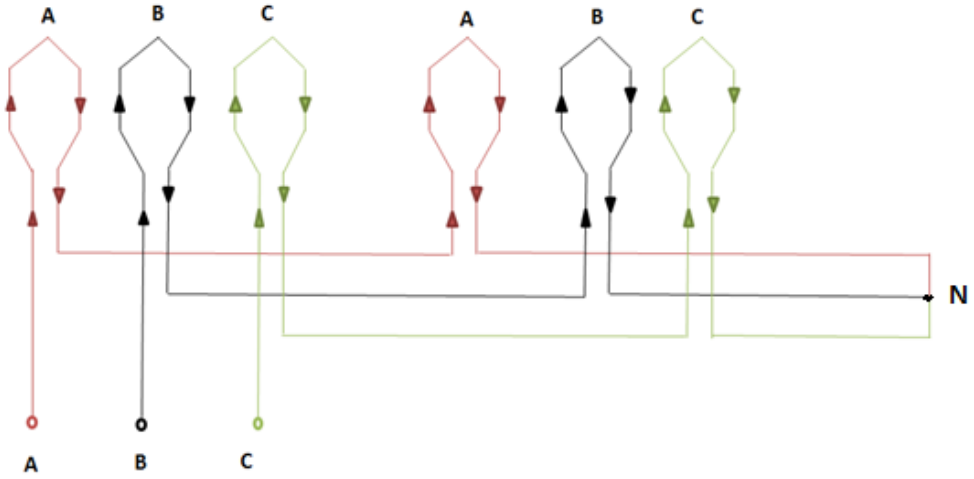


**Figure 5.9 :** Winding scheme.

The last part was the implementation of the hall sensors. The cables for hall sensors are soldered to the breadboard. Figure 5.10 shows the picture of the work done.

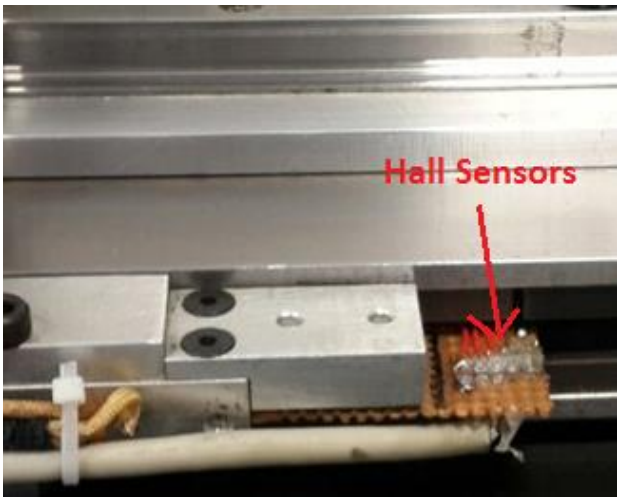


**Figure 5.10:** Motor production detail and hall sensors.

After all the assembly was done, the motor was ready for the tests. The terminal was prepared of the connection of the motor control, so that the unit cables could easily be connected to the linear motor. A finshed model of the motor is shown in Figure 5.11.

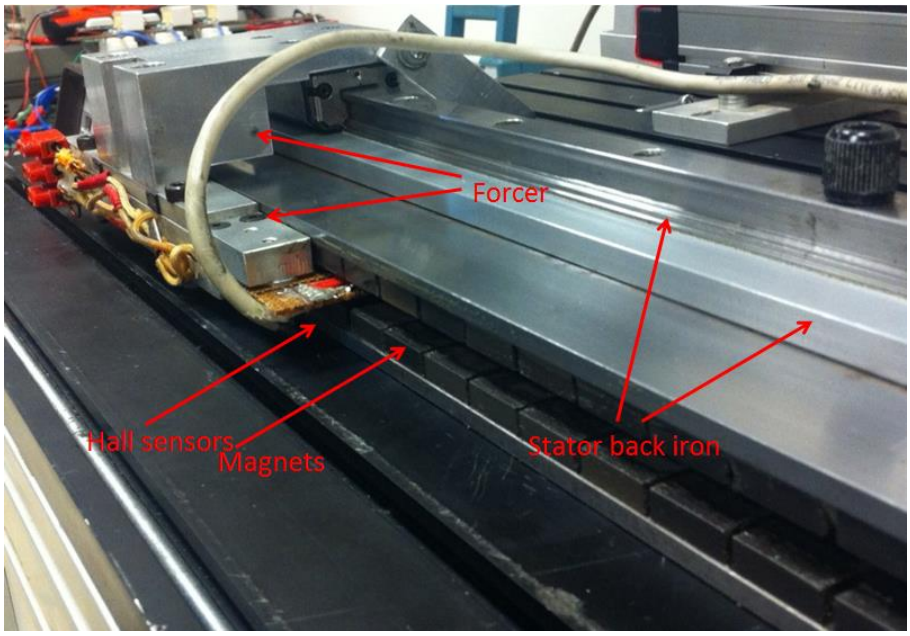


**Figure 5.11 :** Finished linear motor after assembly.

# 6. EXPERIMENTAL STUDY

All experiments are conducted on a test bench with motor fixed in a stable position as shown in Figure 6.1.

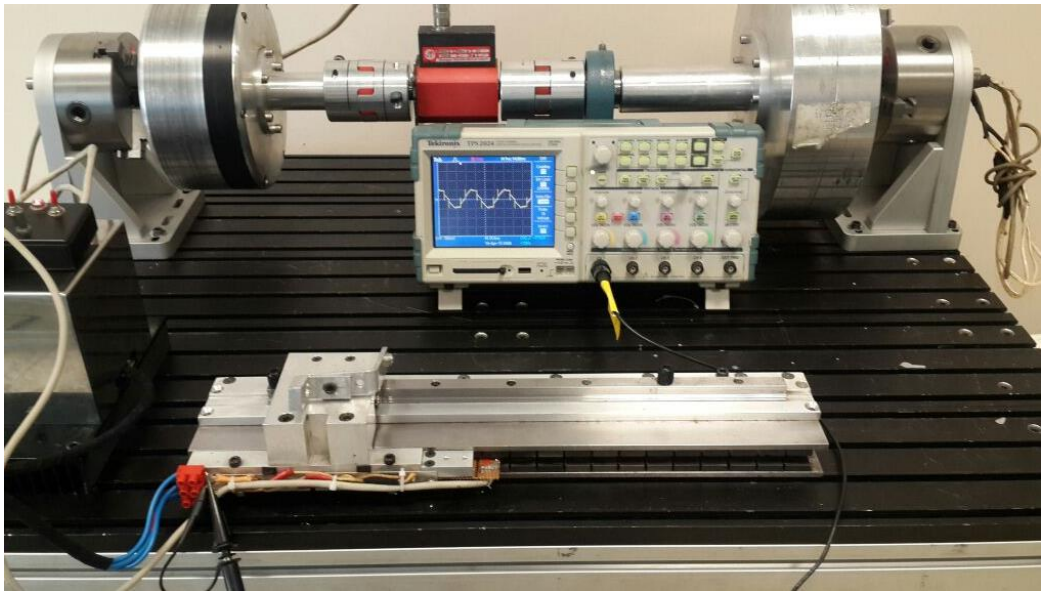

**Figure 6.1 :** Motor test bench.

The initial testing aimed at estimating the current force relation of the motor. To obtain accurate measurements of the force for a given current, the test is repeated three times for each different coil position. Then the motor current and voltage curves are gathered from an oscilloscope in no-load (free running) and loaded conditions of the motor. By using a gaussmeter, electromagnetic field density of each magnet is measured to get an average value of magnetic field density of the magnets, as well as verifying the consistency of the whole structure of the motor. Based on the measured current force relation, the $k\varphi$ value (according to the formula 4.6) of the motor is calculated. Further experiments are performed to identify the wire resistance and inductance. Lastly, the simulaton model is validated by the experimental data.

## 6.1 Testing Force - Current Relation

The first test was to get the current–force curve of the motor under load. For these test runs, the motor is operated at fixed current values ranging from 1A to 20A in 1A

steps. For each current input the corresponding motor force is measured. It shall be emphasized that the tests needed to be conducted in a timely fashion, as the motor heats up quickly under higher loads. Table 6.1 and Figure 6.2 summarize the test results of the motor. The nominal friction of the system and the pull-out force are estimated to be 5N and 5.6N, respectively. This test was repeated three times, each time at a different coil position to ensure consistent measurements and reduce the chance of procedural errors.

**Table 6.1 :** Moving force-current graph results of Test-1.

| Test No. | Current Value (A) | Force Value (N) |
|---|---|---|
| 1 | 1 | 11 |
| 2 | 2 | 12,8 |
| 3 | 3 | 19,8 |
| 4 | 4 | 28,2 |
| 5 | 5 | 36 |
| 6 | 6 | 44,4 |
| 7 | 7 | 52,6 |
| 8 | 8 | 60,6 |
| 9 | 9 | 69,4 |
| 10 | 10 | 77,2 |
| 11 | 11 | 85,2 |
| 12 | 12 | 95 |
| 13 | 13 | 101,6 |
| 14 | 14 | 109,4 |
| 15 | 15 | 117,8 |
| 16 | 16 | 125,8 |
| 17 | 17 | 134,4 |
| 18 | 18 | 142,4 |
| 19 | 19 | 153 |
| 20 | 20 | 161 |

The results of the experiment are shown in Figure 6.2.

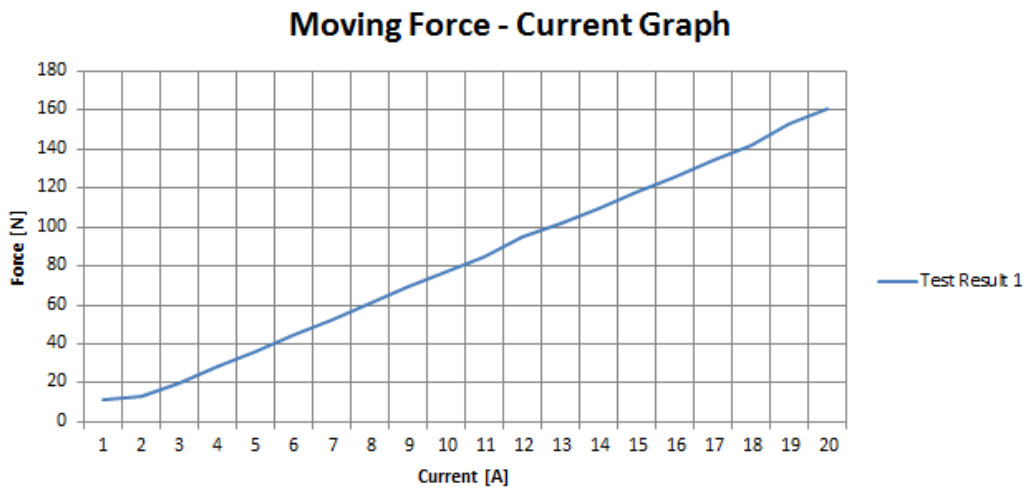


**Figure 6.2 :** Moving force-current graph results of Test-1.

The same test was performed for the second time after changing the position of the coil. The results can be seen in Figure 6.3 and in Table 6.2.

**Table 6.2 :** Moving force-current graph results of Test-2.

| Test No. | Current Value (A) | Force Value (N) |
|---|---|---|
| 1 | 1 | 11 |
| 2 | 2 | 14,2 |
| 3 | 3 | 21,6 |
| 4 | 4 | 30 |
| 5 | 5 | 39 |
| 6 | 6 | 47,4 |
| 7 | 7 | 55,4 |
| 8 | 8 | 64 |
| 9 | 9 | 72,6 |
| 10 | 10 | 81 |
| 11 | 11 | 87,9 |
| 12 | 12 | 97,6 |
| 13 | 13 | 105,8 |
| 14 | 14 | 114 |
| 15 | 15 | 122,8 |
| 16 | 16 | 131,6 |
| 17 | 17 | 140,2 |
| 18 | 18 | 148,6 |
| 19 | 19 | 156,8 |
| 20 | 20 | 163,8 |

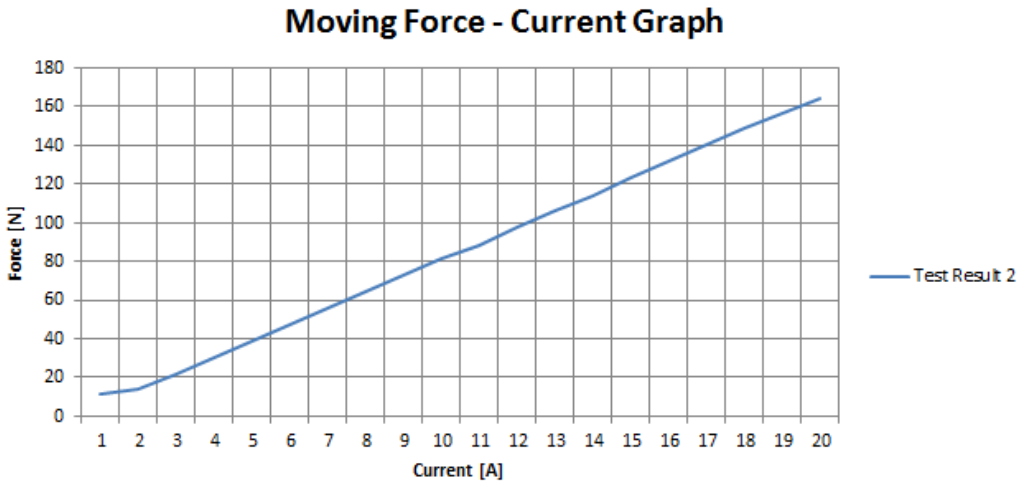


**Figure 6.3 :** Moving force-current graph results of Test-2.

For a third position of the coil the test was performed once again to validate the first two test results.

**Table 6.3 :** Moving force-current graph results of Test-3.

| Test No. | Current Value (A) | Force Value (N) |
|---|---|---|
| 1 | 1 | 11,4 |
| 2 | 2 | 14,4 |
| 3 | 3 | 21,6 |
| 4 | 4 | 30 |
| 5 | 5 | 38,6 |
| 6 | 6 | 47,2 |
| 7 | 7 | 55,6 |
| 8 | 8 | 64,4 |
| 9 | 9 | 73 |
| 10 | 10 | 81,4 |
| 11 | 11 | 89,6 |
| 12 | 12 | 98,4 |
| 13 | 13 | 106,8 |
| 14 | 14 | 115,6 |
| 15 | 15 | 123,8 |
| 16 | 16 | 132,4 |
| 17 | 17 | 140 |
| 18 | 18 | 149,4 |
| 19 | 19 | 158,4 |
| 20 | 20 | 166,6 |

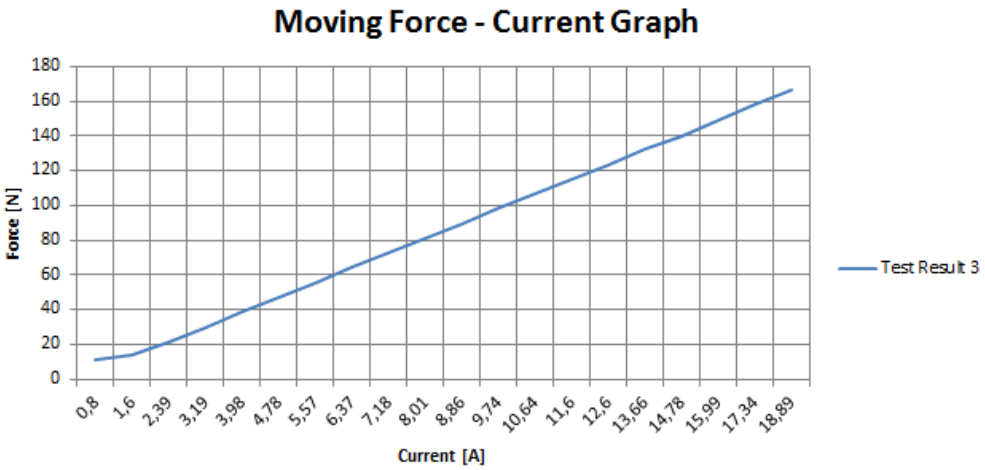


**Figure 6.4 :** Moving force-current graph results of Test-3.

After performing the tests for different positions of the motor, the mean of the three curves was calculated.

**Table 6.4 :** Moving force-current graph, calculated for the average values of the three tests.

| Test No. | Current Value (A) | Average Force Value (N) |
|---|---|---|
| 1 | 1 | 11,13 |
| 2 | 2 | 13,80 |
| 3 | 3 | 21,00 |
| 4 | 4 | 29,40 |
| 5 | 5 | 37,87 |
| 6 | 6 | 46,33 |
| 7 | 7 | 54,53 |
| 8 | 8 | 63,00 |
| 9 | 9 | 71,67 |
| 10 | 10 | 79,87 |
| 11 | 11 | 87,57 |
| 12 | 12 | 97,00 |
| 13 | 13 | 104,73 |
| 14 | 14 | 113,00 |
| 15 | 15 | 121,47 |
| 16 | 16 | 129,93 |
| 17 | 17 | 138,20 |
| 18 | 18 | 146,80 |
| 19 | 19 | 156,07 |
| 20 | 20 | 163,80 |

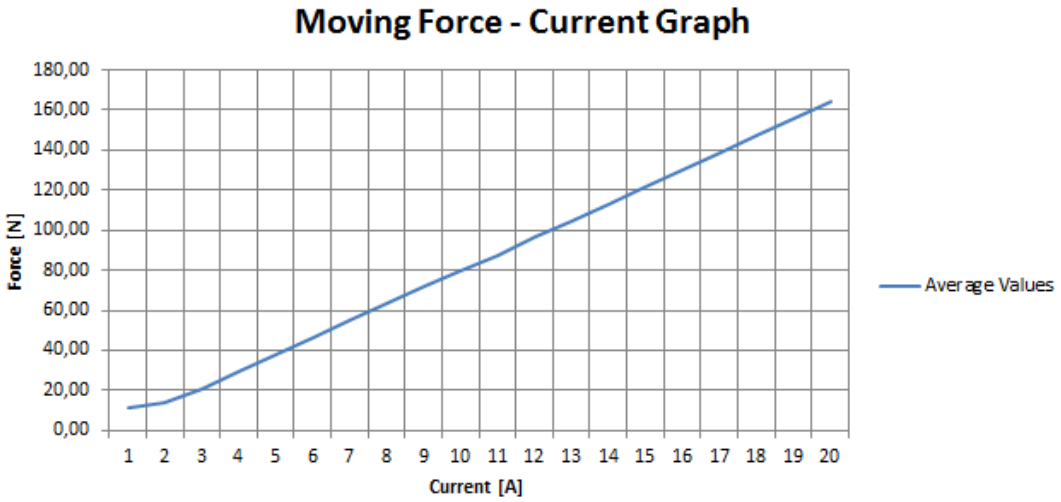


**Figure 6.5 :** Moving force-current graph, plotted for the average values of the three tests.

The experiments show that all three test runs produce consistent measurements within the expected tolerance limit. From the curve, it is visible that force is directly proportional and linear outside the very low current regime.

### 6.2 Motor Free Running Tests

The next set of experiments consist of motor free running tests. No mechanical load is applied to the motor during the experiments. In this section, the measured rotor voltage and current waveforms is shown and investigated The results are captured using an oscilloscope. Only signals in one phase are captured from the oscilloscope. The inverter of the motor drive has a 3V DC source and the switching frequency of the inverter is 10kHz. The reason to select 3V DC is to find a reasonable speed for the motor, so that the results are visible in the oscilloscope. The results are shown in the following figures.

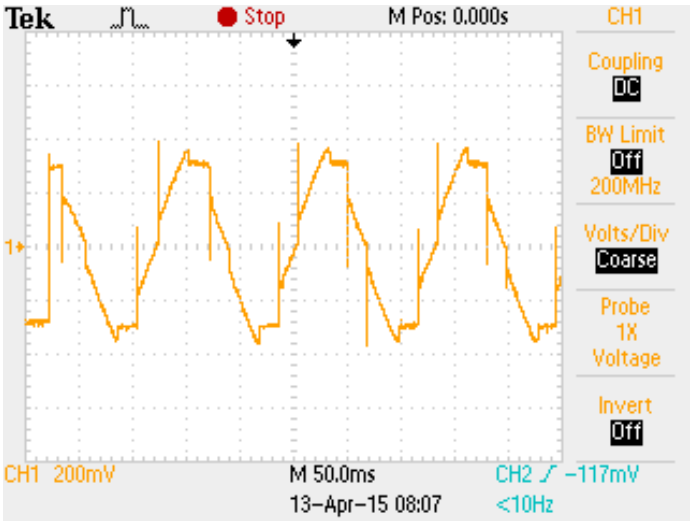


**Figure 6.6 :** Rotor voltage waveform on free running.

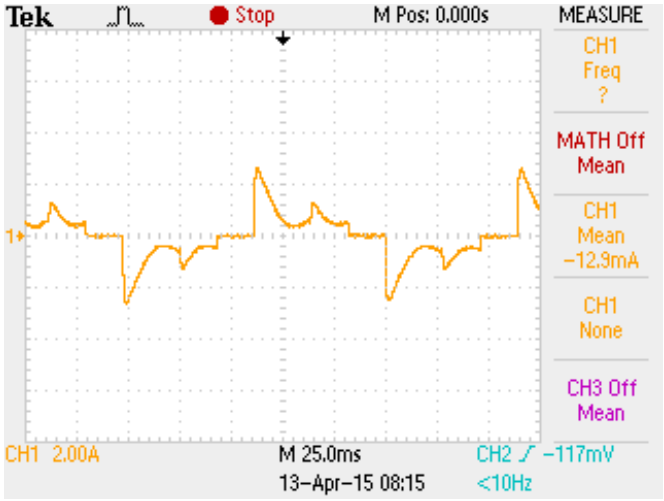


**Figure 6.7 :** Rotor voltage waveform on free running.

The measured peak value of the current is 2.64A.

Chopped tests are also performed. First the PWM signal with the duty cycle of 70% was used to get the current curve without load. Then the PWM duty cycle was increased to 80% to get the voltage waveform for the same condition in free running mode of the motor.

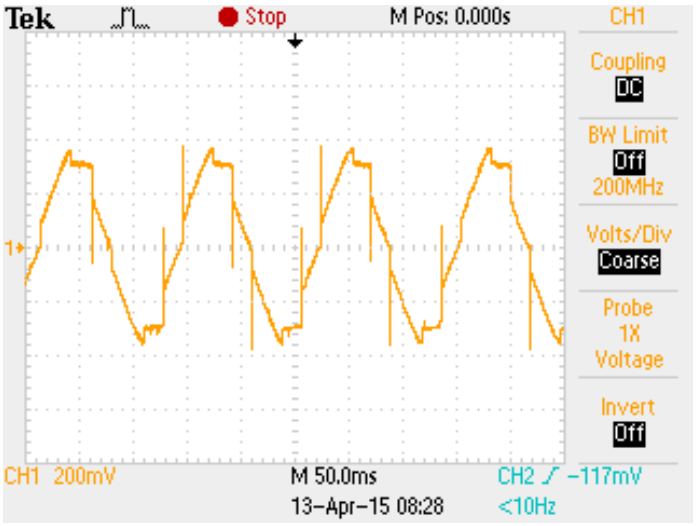


**Figure 6.8 :** Rotor voltage waveform by 80% PWM duty cycle on free running.

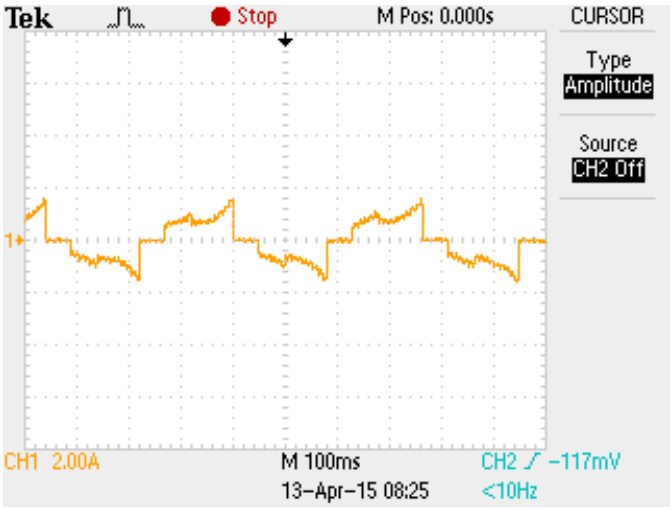


**Figure 6.9 :** Rotor current waveform by 70% PWM duty cycle on free running .

### 6.3 Motor Tests Under Load

After increasing the inverter DC link voltage up to 5V and changing the PWM duty cycle to 100%, the rotor voltage and current waveforms are captured by an oscilloscope. 120 degrees commutation pattern is used to control the motor drive. The spikes occur during the switching of the other two phases.

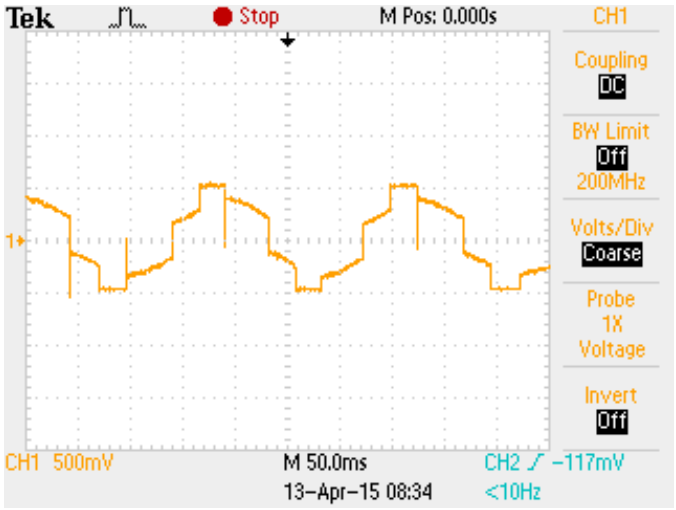


**Figure 6.10 :** Rotor voltage waveform by 100% PWM duty cycle under load.

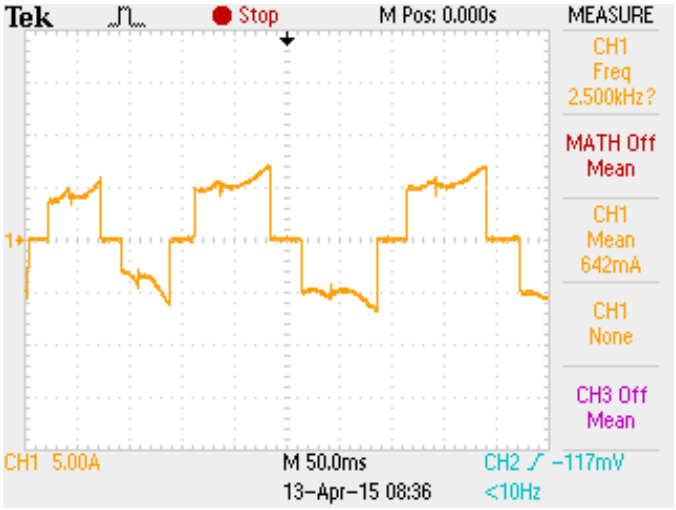


**Figure 6.11 :** Rotor current waveform by 100% PWM duty cycle under load.

The motor under investigation is a PM linear motor with sinusoidal back-emf. To prove this, the back-emf wavefrom is measured during the open circuit voltage test. The fact that rotor voltage waveform by 100% PWM duty cycle under load is not sinusoidal, is due to the effect of excitations provided by the inverter circuit (120 degrees trapezoidal commutation pattern).

### 6.4 Magnetic Field Density of Magnets

Magnetic field density of each magnet is measured by using a gaussmeter as magnets play a big role in a brushless permanent magnet DC motor. The measuring sequence listed in Table 6.5, is chosen in a way that the first value belongs to the most right magnet while the linear motor is resting on its back. A gaussmeter is fixed vertically

in the middle of each magnet to get an accurate value of the magnetic field density. Below is the measured magnetic field values of each magnet from 1 (being the most right) to 22 (being the most left), in Teslas.


**Figure 6.12 :** Measuring magnetic field density of the magnets with a gaussmeter.

**Table 6.5 :** Magnetic field densities of motor magnets.

| Magnet No. | Magnetif Field Density (T) |
|---|---|
| 1 | 0.597 |
| 2 | 0.610 |
| 3 | 0.603 |
| 4 | 0.609 |
| 5 | 0.604 |
| 6 | 0.544 |
| 7 | 0.548 |
| 8 | 0.548 |
| 9 | 0.544 |
| 10 | 0.566 |
| 11 | 0.563 |
| 12 | 0.566 |
| 13 | 0.544 |
| 14 | 0.553 |
| 15 | 0.544 |
| 16 | 0.552 |
| 17 | 0.551 |
| 18 | 0.6 |
| 19 | 0.593 |
| 20 | 0.616 |
| 21 | 0.598 |
| 22 | 0.602 |

The FEM software estimated a field density of 0.7T which matches closely with the measured results. It shall be noted that the FEM software produces the field density exactly at the center of the magnet, whereas the gaussmeter will always have some displacement error due to the manual placement on the magnet. The results show that magnetic field density of all magnets are within an acceptable error tolerance.

### 6.5 Further Tests About Linear Motor

Further tests are conducted to measure the inductance and the resistance of the coils. The wire resistance values of the three phases are measured at 26 degrees Celcius room temperature. The inductances and the resistance values of the coils for three phases are listed in Table 6.6.

**Table 6.6 :** Measured inductance and the resistace values of the coils.

| Phase | Inductance Value (mH) | Resistance Value (mΩ) |
|---|---|---|
| A | 144.5 | 310 |
| B | 131.8 | 290 |
| C | 144.4 | 304 |

### 6.6 Calculating the kφ Value by Using Current-Force Plots

The relationship between the force and the current is given by the following equation:

$$F_e = k \cdot \phi \cdot i \tag{6.1}$$

The output force is the difference between electrical force and the pull-out force.

$$F_{out} = F_e - F_{pull-out} \tag{6.2}$$

The pull-out force is calculated as 5.6N as stated previously in this chapter.

Starting from 10A, the $k\varphi$ values are calculated for each current-force result pair. The average value of the $k\varphi$'s from the 10 results are calculated again. The average value of $k\varphi$ is 8,48.

### 6.7 Comparing Test Results with Simulation Results

Below is a comparison to show the consistency of the simulation model with the experimental data. The right side shows the average values measured over all test runs and in the middle column the corresponding forces of the simulation model are listed.

**Table 6.7 :** Comparison between test and simulation results on force.

| Current Values [A] | Calculated Force Values from Simulations[A] | Average Force Value from Test Resuls[N] |
|---|---|---|
| 10 | 80,4981 | 79,87 |
| 11 | 90,0268 | 87,57 |
| 12 | 92,8170 | 97,00 |
| 13 | 100,7430 | 104,73 |
| 14 | 109,0523 | 113,00 |
| 15 | 130,8002 | 121,47 |
| 16 | 135,6024 | 129,93 |
| 17 | 140,5841 | 138,20 |
| 18 | 145,2559 | 146,80 |
| 19 | 153,2346 | 156,07 |
| 20 | 161,2133 | 163,80 |

The difference in the force values are between 1% and 7%. This is an acceptable difference. There are several factors that contribute to this mismatch. For instance, the mesh, the time step size or the non-linear material properties all have an impact on the outcome of the simulation. Refining any of these may lead to a better match of the simulation model with the experimental data.

# 7. CONCLUSIONS AND RECOMMENDATIONS

In this chapter, conclusion is briefly given and to improve the performance of the coreless double-sided linear motor future works are discussed.

## 7.1 Conclusion

In the last decade, research on linear motors is getting more and more important. They are capable of many significant applications such as precision positioning and robotics. Linear motors are designed to produce high force at low speeds and the sizing is not based on power but purely on force.

The research considers the linear motor itself and the control circuit. As part of the studies, a linear motor is designed (based on existing magnets) and built, then its behavior is investigated.

High precision is the primary application for the proposed linear motor. It can also provide fast, forceful actuation from a compact volume. The study considers a short stroke motor. A short stroke motor gives high precision when having double sides and an air-core. As a result, a coreless double-sided linear motor has been chosen because of its advantages and providing the needed force in a short stroke configuration. An air-core provides smooth movement. Double sides help the motor work at very high and very low speeds and accelerate faster.

First, the design of the geometry is created considering the technical requirements and existing magnets (NdFeB). Then, the motor is designed in a FEA software. A small hand calculation is made to verify the FEM analyses results. After proving the FEA results, all the simulations are performed. The materials are selected according to motor needs. The linear motor is produced and assembled after the successful competition of the simulations and based on CAD drawings. The production is followed by the laboratory tests. Test results are compared with FEA results and it is shown that the simulations adequately represent the motor behavior. Tests show that motor can be used in precise motion with high force production. It is also proved that

FEM analysis gives a good approach to design a linear motor. This completes the study of the research.

### 7.2 Future Works and Recommendations

In the thesis, the functionality of the design has been experimentally validated. The next step shall be to modify the system to achieve better results. The motor performance can be improved in many areas, e.g., noise. Noise prevents the motor from being useful for applications that require precise positioning when the amplitude is high. To overcome this problem, another sensor can be introduced that has a finer position resolution. This step should greatly increase the motor's usefulness to precision positioning applications.

Another significant problem in the system is the heating of the motor under load. Controlling the heat problem could allow significally faster, better performance and will allow the motor to run longer.

.

## REFERENCES


**[1] Basak, Amitava,** (1996) Permanent Magnet DC Linear Motors, Clarendon Press, Oxford, Cardiff School of Engineering, University of Wales College of Cardiff.

**[2] Buasre, A., Subsingha, W.,** (2012). Double-Sided Linear Induction Motor Control Using Space Vector Pulse Width Modulation Technique, *10th Eco-Energy and Materiasls Science and Engineering Conference*, Rajamngala University of Technology Thanyaburi, Lanna Nan, Thailand.

**[3] Cao, R., Cheng, M., Hua, W.,** (2013) Investigation and General Design Principle of a New Series of Complementary and Modular Linear FSPM Motors, Members of IEEE, 12 Dec 2013.

**[4] Cao, R., Huang, W., Cheng, M.,** (2014). A New Modular and Complementary Double-Sided Linear Flux-Switching Permanent Magnet Motor with Yokeless Secondary, *17h International Conference on Electrical Machnes and Systems* Department of Electrical Engineering, Nanjing University of Aeronautics and Astronauutics, Nanjing, China, School of Electrical Engineering, Souteast University, China, 22-25 Oct 2014.

**[5] Caruso, M., Cipriani, G., Di Dio, V., Miceli, R., Spataro, C.,** (2014). Speed Control of Double-Sided Linear Induction Motors for Automated Manufacturing Systems, *ENERGYCON 2014*, Dubrovnik, Crotia, 13-16 May 2014.

**[6] Chiang, H.-H., Hsu, K.-C.,** (2015). Optimized Adaptive Motion Control Through an SoPC Implementation of Linear Induction Motor Drives, IEEE Members, 1 Feb 2015.

**[7] Chung, M.-J., Gweon, D.-G.,** (2003). Design Optimization and Development of Linear Brushless Permanent Magnet Motor, *International Journal of Control, Automation, and Systems* (Vol.1, No.3), 3 Sep 2003.

**[8] Daldaban, F., Ustkoyuncu, N.,** (2006). A New Double Sided Linear Switched Reluctance Motor with Low Cost, Erciyes University, Faculty of Engineering, Department of Electrical and Electronics Engineering, Kayseri, Melikgazi, Turkey,22 May 2006.

**[9] Darabi, A., Ghanaee, R., Shariati, A., Siahi, M.,** (2013). Efficiency Maximization of the Air Core Double-Sided Permanent Magnet Linear Synchronous Motor, Electrical Engineering Department, Azad University, Garmsar Branch, Garmsar, Iran.

**[10] Dr., McLean, G., W.,** (n.d) Review of recent progress in linear motors.

**[11] Dr., Perrault, B., M.,** (n.d) Control Strategies for Linear Synchronous Motors

**[12] Huang, L., Yu, H., Hu, M., Liu, Hexiang, L.,** (2013). Study on a Long Primary Flux-Switching Permanent Magnet Linear Motor for Electromagnetic Launch Systems, *IEEE Transactions on Plasma Science* (Vol.41, No.5), 5 May 2013.

**[13] Isfahani, A., H.,** (2010). Analytical Framework for Thrust Enhancement in Permanent-Magnet (PM) Linear Synchronous Motors with Segmented PM Poles, Islamic Azad University, Khomeinishahr Branch, Isfahan, Iran.

**[14] Jin, X., Xidang, Y., Weiming, M., Yuexing, Z., Zhaolong, S.,** (2014). Nonlinear Calculation Methods of Long Primary Double-Sided Linear Induction Motor *17h International Conference on Electrical Machines and Systems* Institute of Power Electronics Technology, Naval University of Engineering, China, 22-25 Oct 2014.

**[15] Jin, X., Xidang, Y., Weiming, M., Yuexing, Z., Zhaolong, S.,** (n.d) The Mathematical Model and Performance Analysis of a Novel Four-stator Double-Sided Linear Induction Motor, Naval University of Engineering, China.

**[16] Kenjo and Nagaromi,** (1985), Permanent-Magnet and Brushless DC Motors, Clarendon Press, Oxford

**[17] Kim, J.-J., Jeong, Y., H., Cho, D.-W.,** (2004). Thermal Behavior of a Machine Tool Equipped with Linear Motors, iCurie-Lab, Seul, South-Korea, Department of Mechanical Engineering, Pohang University of Science and Technology, Nan.gu, Pohang, South Korea, 2 Feb 2004.

**[18] Liu, Q., Zhang, R., Du, Y., Shi, L., Li, Y.,** (2014) Performance Comparison of Control Methods for High Speed Long Primary Double-Sided Linear Induction Motor *17h International Conference on Electrical Machines and Systems* Key Laboratory of Power Electronics and Electric Drive, Institute of Electrical Engineering, Chinese Academy of Sciences, China, University of Chinese Academy of Sciences, China, 22-25 Oct 2014.

**[19] Manno, R., H., Diez, E., G.,** (n.d) Direct Force Control for a Three-Phase Double-Sided Linear Induction Machine With Transverse Magnetic Flux, Facultad de Ingenieria, Universidad Nacional de Rio Cuarto, Rio Cuarto, Argentina, Dpto. Ingenieria Electronica, Universidad de Sevilla, Sevilla, Spain.

**[20] Minghu, Y., Yuqiu, Z., Xiao, L., Yunyue, Y.,** (2010). Design Method and Analysis of Double-Side Air-Core Permanent Magnet Linear Servo Motor, *Electrical Machines and Systems (ICEMS), 2010 International Conference,* College of Electrical Engineering, Zhejiang University, Hangzhou, China.

**[21] Mirsalim, M., Doroudi, A., Moghani, J., S.,** (2002). Obtaining the Operating Characteristics of Linear Induction Motors: A New Approach, IEEE Members, 2 Mar 2002.

**[22] Naso, D., Cupertino, F., Turchiano, B.,** (2010). Precise Position Control of Tubular Linear Motors with Neural Networks and Composite

Learning, Dipartimento di Elettrotecnica ed Elettronica, Politecnico di Bari, Bari, Italy, 18 Feb 2010.

**[23] Pluk, K., J., W., Jansen, J., W, Lomonova, E., A.,** (2014). Force Measurements on a Shielded Coreless Linear Permanent Magnet Motor, Department of Electrical Engineering , Eindhoven University of Technology, Eindhoven, Netherlands, 11 Nov 2014.

**[24] Rothenhoefer, G., Slocum, A.,** (2008). Reducing Pitch Error of a Linear Motion System Actuated by a Permanent Magnet Open Face Linear Motor, Massachusets Institute of Technology, Cambridge, MA, USA, 13 Sep 2008.

**[25] Sato, K.,** (2014). High-Precision and High-Positioning of 100 G Linear Synchronous Motor, Interdisciplinary Graduate School of Science and Engineering, Tokyo Institute of Technology Yokohana, Japan.

**[26] Shiri, A., and Shoulaie, A.,** (2012). End Effect Breaking Force Reduction in High-Speed Single-Sided Linear Induction Machine, Electrical Engineering Department, Iran University of Science and Technology, Tehran, Iran.

**[27] Sotelo, G., G., de Oliveira, R., A., H., Costa, F., S., Dias, D., H., N., de Andrade, Jr., R., Stephan, R., M.,** (2015). A Full Scale Superconducting Magnetic Levitation (MagLev) Vehicle Operational Line, *IEEE Transactions on Applied Superconductivity* (Vol.25, No.3), 3 June 2015.

**[28] Srivastava, R., K.,** (2001). Characteristic of Double Gap SLIM under Constant Current Excitation. Department of Electrical Engineering, Institute of Technology, Banaras Hindu University, Varanasi, India, 1 Mar 2001.

**[29] Üstün, Ö., Kömürgöz. G., Tuncay, N., R.,** (n.d.). Sürekli Mıknatıslı Demir Çekirdeksiz Lineer Fırçasız Doğru Akım Motoru Tasarımı, Elektrik-Elektronik Fakültesi, Elektrik Mühendisliği Bölümü, Elektrik Makinaları Ana Bilim Dalı.

**[30] Ustun, O., Tuncay, R., N.,** (2006.). Design, Analysis and Control of A Novel Linear Actuator, Electrical and Electronics Faculty, Electrical Engineering Department, Maslak, Istanbul, 17 July 2006.

**[31] Yang, T., Zhou, L., Li, L.,** Performance Calculation for Double-Sided Linear Induction Motor with Short Secondary, College of Electrical and Electronic Engineering, Huazhong University of Science and Technology, Wuhan, China.

**[32] Yuqiu, Z., Minghu, Y., Yunyue, Y., Xiao, L.,** (2010). Computer Simulation Study on Optimization of Linear Servo Motor Used in CNC Machines, College of Electrical Engineering, Zhejiang University, Hangzhou, China.

**[33] Zheng, L., Jin, J., Guo, Y., Zhu, Jianguo** (2007). Design of an HTS Levitated Double-Sided HTSLSM for Maglev *Superconductivity Centennial Conference*, University Technology Sydney, University of Electronic Science and Technology of China.

**[34] Zhu, Y., Cho, Y.,** (2010). Structure Selection of Permanent Magnet Linear Synchronous Motor for Ropeless Elevator System, Power Electronics Application Lab, Faculty of Electrical Engineering, Dong-A University, Pusan, Korea.

**[35] Zhu, Y., Lee, S., Cho, Y.,** (2010). Topology Structure Selection of Permanent Magnet Linear Synchronous Motor for Ropeless Elevator System, Electrical Engineering, Dong-A University, Busan, Korea.

**[36] BH Curve of Steel_1010 Material..** (n.d.). In *ANSYS Maxwell Online Help*. Date retrieved: 25.02.2015

**[37] Url-3** <*http://oytunyapici.net*>, date retrieved 05.04.2015

**[38] Url-4** <*http://www.explainthatstuff.com*>, date retrieved 14.03.2015

**[39] Url-5** <*http://www.magnetictransportsystems.com*>, date retrieved 14.03.2015

**[40] Url-7** <*http://derstandard.at*>, date retrieved 21.04.2015

**[41] Url-8** < *http://en.wikipedia.org*>, date retrieved 25.04.2015

**[42] Url-9** <*http://www.productionmachining.com*>, date retrieved 25.04.2015

**[43] Url-10** <*http://machinedesign.com*>, date retrieved 25.04.2015

**[44] Url-11** <*http://onlinecatalog.tpa-us.com*>, date retrieved 25.04.2015

**[45] Url-12** <*http://www.etel.ch*>, date retrieved 28.04.2015

**[46] Url-13** <*https://www.yumpu.com*>, date retrieved 28.04.2015

**CURRICULUM VITAE**

**Name Surname: Özge Taskin**

**Place and Date of Birth: Sakarya – 07/05/1984**

**Address: Gewerbering 6 83624 Munich**

**E-Mail: ozgemis@gmail.com**

**EDUCATION: BSc. Electrical Engineering**

**B.Sc.:Electrical Engineering**

**PROFESSIONAL EXPERIENCE AND REWARDS:**

**ANSYS Germany GmbH (Otterfing, Germany)**
(September 2011 - Present)
*Technical Suupport Engineer I*
Working as a technical support engineer, supporting low frequency electromagnetic products. Giving both in house and on site trainings as well as contributing pre-sales activities.

**FIGES Engineering (Istanbul, Turkey)**
(August 2010 – August 2011)
*Electromagnetic Analysis and Application Engineer*
Worked as an application and consulting engineer to support electromagnetic products. Carried two projects for the defense industry.

**AGRA Electric Limited (Istanbul, Turkey)**
(November 2009 – August 2010)
*Project Engineer*
Worked as a design engineer, desiging middle voltage switchgear board circuits.

**EATON Corporation (Istanbul, Turkey)**
(September 2007 – November 2009)
*Product Manager*
*Project Sales Engineer*
Started as a slaes engineer for switch gear board products. Became a product manager for smart house equipments.